THE GEOLOGICAL SOCIETY OF AMERICA®

Deposition and age of Chicxulub impact spherules on Gorgonilla Island, Colombia

Paula Mateo[1,†], Gerta Keller[2], Thierry Adatte[3], André M. Bitchong[4,5], Jorge E. Spangenberg[6], Torsten Vennemann[6], and Christopher J. Hollis[7]

[1]*Division of Geological and Planetary Sciences, California Institute of Technology, Pasadena, California 91125, USA*
[2]*Department of Geosciences, Princeton University, Princeton, New Jersey 08544, USA*
[3]*Institute of Geology and Paleontology, University of Lausanne, Lausanne 1015, Switzerland*
[4]*Department of Earth Sciences, Faculty of Science, University of Yaounde 1, Yaounde, Cameroon*
[5]*Department of Petroleum and Gas Exploration, Institute of Mines and Petroleum Industries, University of Maroua, Kaele, Cameroon*
[6]*Institute of Earth Surface Dynamics (IDYST), University of Lausanne, Lausanne 1015, Switzerland*
[7]*GNS Science, Lower Hutt, 5040, New Zealand*

ABSTRACT

The end-Cretaceous mass extinction (66 Ma) has long been associated with the Chicxulub impact on the Yucatan Peninsula. However, consensus on the age of this impact has remained controversial because of differing interpretations on the stratigraphic position of Chicxulub impact spherules relative to the mass extinction horizon. One side argues that the impact occurred precisely at the Cretaceous-Paleogene boundary, thus coinciding with the mass extinction; the other side argues that the impact predated the Cretaceous-Paleogene boundary, based on the discovery of primary impact spherules deposits in NE Mexico and Texas near the base of planktic foraminiferal zone CF1, dated at 170 k.y. before the Cretaceous-Paleogene boundary. A recent study of the most pristine Chicxulub impact spherules discovered on Gorgonilla Island, Colombia, suggested that they represent a primary impact deposit with an absolute age indistinguishable from the Cretaceous-Paleogene boundary. Here, we report on the Gorgonilla section with the main objective of evaluating the nature of deposition and age of the spherule-rich layer relative to the Cretaceous-Paleogene boundary.

The Gorgonilla section consists of light gray-yellow calcareous siliceous mudstones (pelagic deposits) alternating with dark olive-brown litharenites (turbidites). A 3-cm-thick dark olive-green spherule-rich layer overlies an erosional surface separating Maastrichtian and Danian sediments. This layer consists of a clast-supported, normally graded litharenite, with abundant Chicxulub impact glass spherules, lithics (mostly volcanic), and Maastrichtian as well as Danian microfossils, which transitions to a calcareous mudstone as particle size decreases. Mineralogical analysis shows that this layer is dominated by phyllosilicates, similar to the litharenites (turbidites) that characterize the section. Based on these results, the spherule-rich layer is interpreted as a reworked early Danian deposit associated with turbiditic currents. A major hiatus (>250 k.y.) spanning the Cretaceous-Paleogene boundary and the earliest Danian is recorded at the base of the spherule-rich layer, based on planktic foraminiferal and radiolarian biostratigraphy and carbon stable isotopes. Erosion across the Cretaceous-Paleogene boundary has been recorded worldwide and is generally attributed to rapid climate changes, enhanced bottom-water circulation during global cooling, sea-level fluctuations, and/or intensified tectonic activity. Chicxulub impact spherules are commonly reworked and redeposited into younger sediments overlying a Cretaceous-Paleogene boundary hiatus of variable extent in the Caribbean, Central America, and North Atlantic, while primary deposits are rare and only known from NE Mexico and Texas. Because of their reworked nature, Gorgonilla spherules provide no stratigraphic evidence from which the timing of the impact can be inferred.

INTRODUCTION

The end-Cretaceous mass extinction (66 Ma) is one of the five major biotic crises in Earth's history, and since 1980, it has been attributed to a meteorite impact (Alvarez et al., 1980) related to the impact crater (Chicxulub) discovered on the Yucatan Peninsula (Hildebrand et al., 1991; review in Schulte et al., 2010). Ever since the discovery of the Chicxulub crater, impact spherules at or near the Cretaceous-Paleogene boundary in Mexico, the Caribbean, Central America, the United States, and the North Atlantic have become major players in solving the age of the impact relative to the mass extinction based on their stratigraphic positions. However, consensus on the age of the Chicxulub impact has remained controversial, primarily because of differing interpretations regarding these impact deposits, with one side arguing that the impact occurred precisely at the Cretaceous-Paleogene boundary, thus coinciding with the mass extinction (review in Schulte et al., 2010), and the other side arguing that the impact predated the Cretaceous-Paleogene boundary (Keller et al., 2004a, 2009a; review in Keller, 2011).

The discovery of the Cretaceous-Paleogene boundary mass extinction in planktic foraminifera between major Deccan eruptions in India (Keller et al., 2011a, 2012) and recent studies pointing to Deccan volcanism as an important contributor to environmental stress across the Cretaceous-Paleogene boundary (e.g., Font et al., 2016; Keller et al., 2016; Punekar et al., 2014a; Schoene et al., 2015, 2019) have revived the mass extinction debate challenging a Cretaceous-Paleogene boundary role for the Chicxulub impact.

When did the Chicxulub impact occur relative to the Cretaceous-Paleogene boundary? What was its contribution to the Cretaceous-Paleogene boundary mass extinction? To answer these questions, the study of impact deposits that can be evaluated both stratigraphically (i.e., relative

†pmateo@caltech.edu

GSA Bulletin; January/February 2020; v. 132; no. 1/2; p. 215–232; https://doi.org/10.1130/B35287.1; 15 figures; 1 table; Data Repository item 2019245; published online 17 June 2019.

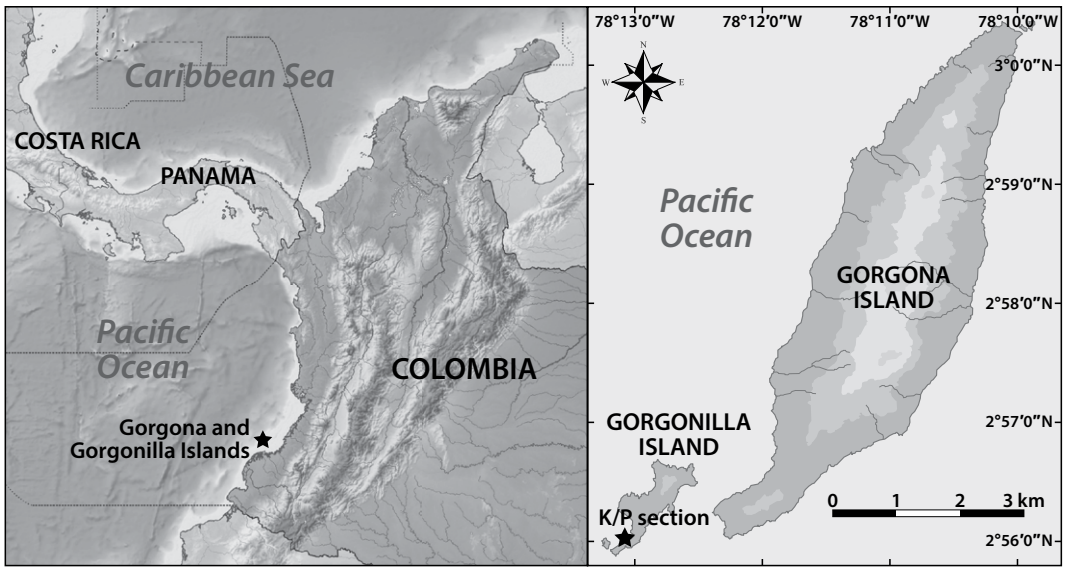

Figure 1. Location of the Cretaceous–Paleogene (K/P) section and Chicxulub impact spherules on Gorgonilla Island, Colombia.

timing of events) and geochronologically (i.e., absolute age of the impact) is imperative.

A recent study of the most pristine Chicxulub impact spherules discovered on Gorgonilla Island, Colombia, suggested that they represent a primary impact deposit with an absolute age indistinguishable from the Cretaceous-Paleogene boundary, based on $^{40}Ar/^{39}Ar$ dating (Renne et al., 2018). Here, we report on the Gorgonilla section with the main objective of evaluating the nature of deposition and age of the spherule-rich layer relative to the Cretaceous-Paleogene boundary. Methods included: (1) lithological analysis to assess the sedimentary processes that deposited the spherule-rich layer, (2) planktic foraminiferal and radiolarian biostratigraphy to estimate the relative age of this deposit, (3) bulk-rock carbon and oxygen stable isotope analyses to evaluate environmental changes and continuity of sediment deposition, and (4) bulk-rock mineralogy to assess sediment sources.

MATERIALS AND METHODS

Gorgonilla Island (2°56′N, 78°12′W) is located in the eastern Pacific Ocean 50 km west of the coast of Colombia (Fig. 1). Along with Gorgona Island, Gorgonilla is considered to have been formed in the Late Cretaceous (ca. 90 Ma; Kerr and Tarney, 2005; Storey et al., 1991) in association with the Caribbean large igneous province in an oceanic slab window setting (Serrano et al., 2011). These islands represent the last fragment of the Caribbean large igneous province accreted to northern South America in the Eocene (Kerr and Tarney, 2005; Kennan and Pindell, 2009). Mafic and ultramafic rocks (e.g., basalts, gabbros, peridotites) and pyroclastic deposits outcrop along their coasts. Paleomagnetic studies indicate that the islands were originally formed at a paleolatitude of 26°S (Estrada and MacDonald, 1994), and, by the time of the Chicxulub impact, they were located ~3000 km southwest of the impact site (Bermúdez et al., 2016).

The Cretaceous–Paleogene section outcrops on the beach on the southwest coast of Gorgonilla Island as a sequence of pelagic sedimentary beds intercalated with turbiditic deposits (Fig. 2A). A thin spherule-rich layer interpreted as a Chicxulub impact deposit separates Cretaceous and Paleogene sediments (Bermúdez et al., 2016).

In total, 103 samples were collected every 20 cm, on average, from 15.6 m below the Cretaceous-Paleogene boundary to 6.3 m above it. At least one sample was collected from each bed in this sedimentary sequence, and the Cretaceous-Paleogene transition was sampled at a higher resolution.

The oxygen isotope composition (^{16}O, ^{18}O) of glass spherules was measured at the University of Lausanne, Switzerland, using a method similar to that described in Vennemann et al. (2001). Between 0.5 and 2 mg aliquots of a sample were loaded onto a small Pt-sample holder and pumped out to a vacuum of ~10^{-6} mbar. After preflourination of the sample chamber overnight, the samples were heated with a CO_2 laser in 50 mbar of pure F_2. Excess F_2 was separated from the O_2 produced by conversion to Cl_2 using KCl held at 150 °C. The extracted O_2 was collected on a molecular sieve (5A) and expanded into the inlet of a Finnigan MAT 253 isotope ratio mass spectrometer. Oxygen isotope compositions are given in the standard δ notation, expressed relative to Vienna standard mean ocean water (VSMOW) in per mil (‰). Replicate oxygen isotope analyses of the standard NBS-28 quartz ($n = 3$) had a precision of ±0.1‰ for $\delta^{18}O$. The accuracy of $\delta^{18}O$ values was better than 0.2‰, compared to accepted $\delta^{18}O$ values for NBS-28 of 9.64‰.

Oxygen and carbon isotope analyses of carbonates were performed on bulk rock at the University of Lausanne, Switzerland, using a Thermo Fisher Scientific GasBench II connected to a Thermo Fisher Scientific Delta Plus XL mass spectrometer, in continuous He-flow mode, following the procedure described in Spötl and Vennemann (2003). Isotope compositions are given in the standard δ notation, expressed relative to Vienna Peedee belemnite (VPDB) in per mil (‰). Analytical uncertainty (2σ) monitored by replicate analyses of the international calcite standard NBS-19 ($\delta^{13}C$ = +1.95‰, $\delta^{18}O$ = –2.20‰) and the laboratory standard Carrara Marble ($\delta^{13}C$ = +2.05‰, $\delta^{18}O$ = –1.70‰) was better than ±0.05‰ for $\delta^{13}C$ and ±0.1‰ for $\delta^{18}O$ values. The corresponding data table is available as supplementary material (Table DR1).[1]

Bulk-rock mineralogy was determined by X-ray diffraction (XRD; Xtra ARL Diffractometer) at the University of Lausanne, Switzerland, based on procedures described by Kübler (1987) and Adatte et al. (1996). The semiquantification of whole-rock mineralogy was based on XRD patterns of random powder samples (~800 mg aliquots of each rock powder were pressed in a powder holder, covered with a blotting paper, and analyzed by XRD) by using exter-

[1]GSA Data Repository item 2019245, carbon and oxygen stable isotopes and mineralogy data tables and radiolarian species plate, is available at http://www.geosociety.org/datarepository/2019 or by request to editing@geosociety.org.

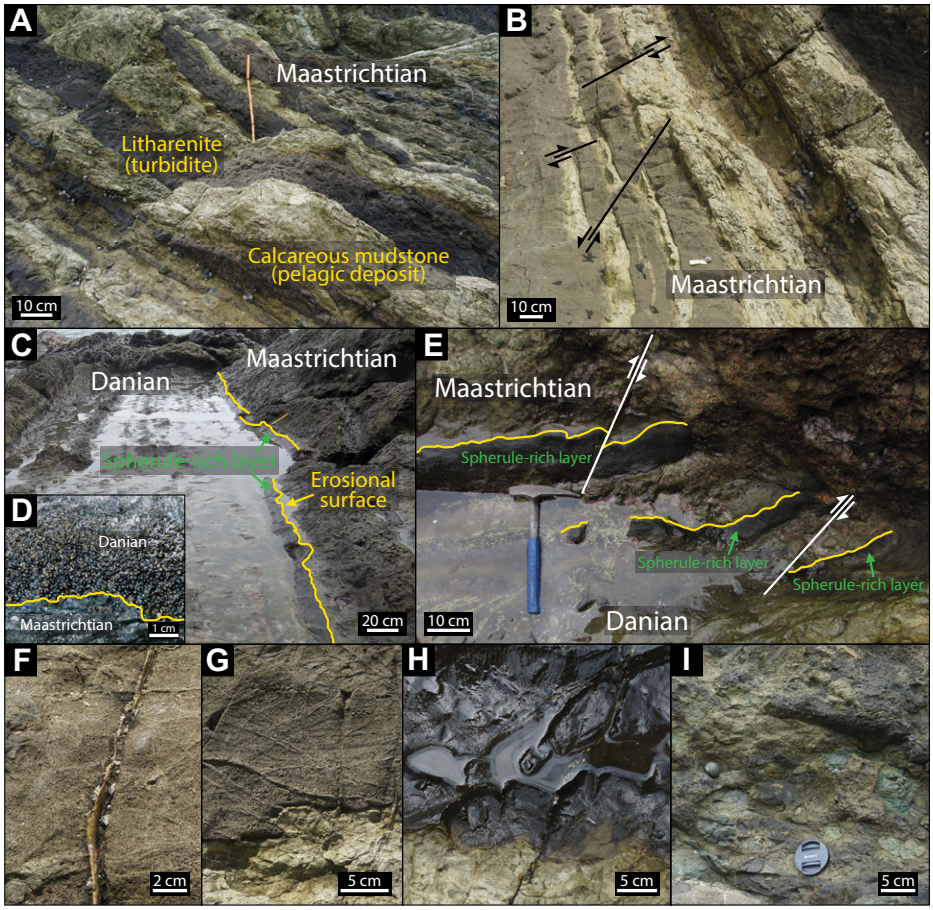

Figure 2. Cretaceous–Paleogene (K/P) outcrops on Gorgonilla Island, Colombia. (A) Cretaceous–Paleogene sequence consists of pelagic sedimentary beds (light gray-yellow calcareous mudstones) alternating with turbiditic deposits (dark olive-brown litharenites). (B) Syn- and postdepositional faulting and folding were observed over the entire sequence from the late Maastrichtian to the early Danian. (C, D) Overlying an erosional surface, a dark olive-green, normally graded, spherule-rich layer separates Maastrichtian and Danian sediments (photo credit: Hermann Bermúdez). (E) Minor syndepositional slumping and postdepositional faulting led to the triplication of the spherule-rich layer at one edge of the outcrop. (F, G) Normal gradation and sorting and (H) irregular bases generally characterize the turbiditic deposits. (I) Some turbidites in the late Maastrichtian section show poorly sorted, structureless sediments above an erosional surface indicating higher dynamic conditions.

nal standards with an error of 5%–10% for the phyllosilicates and 5% for grain minerals. The corresponding data table is available as supplementary material (Table DR2, see footnote 1).

Planktic foraminiferal analyses were performed at Princeton University using washed residues and thin sections where the lithology was indurated enough to resist disaggregation. Identification of species was based on standard taxonomic concepts (Robaszynski et al., 1983–1984; Nederbragt, 1991; Olsson et al., 1999). For washed residues, samples were processed in the laboratory following the procedure described in Keller et al. (1996). Samples were soaked overnight in 3% hydrogen peroxide solution to oxidize organic carbon. After disaggregation of sediment particles, samples were washed through 63 µm and 38 µm sieves to obtain clean foraminiferal residues. Washed residues were oven dried at 50 °C. Planktic species analyses were performed on the 38–63 µm and >63 µm size fractions. All specimens were identified and mounted on microslides for a permanent record.

Radiolarian analyses were performed at GNS Science, New Zealand. Samples were processed using standard methods for siliceous sediments. Samples were first crushed into pieces of 5 mm diameter and leached in 10% hydrochloric acid to remove carbonate. Then, samples were rinsed and placed in 5% hydrofluoric acid for 4–8 h. Sample residues were separated from the larger rock fragments and cleaned by gentle boiling in a solution of 10% hydrogen peroxide and Calgon. Clean residues were washed through a 63 µm sieve, oven dried at 60 °C, and then mounted on glass slides using Canada balsam mounting medium. Radiolarians were identified, and representative specimens were photographed using a Leitz Ortholux transmitted light microscope mounted with an OptixCam digital camera.

RESULTS

Lithology

At Gorgonilla, the Cretaceous–Paleogene section consists of light gray-yellow calcareous siliceous mudstones alternating with dark olive-brown litharenites (Fig. 2A). Deposition occurred in a lower bathyal slope environment at or below the lysocline, as inferred by the absence of bioturbation, presence of bathyal benthic foraminifera (e.g., *Nuttallides truempyi*), and poor preservation of planktic foraminifera. The entire sequence from the late Maastrichtian to the early Danian is strongly disturbed by syn- and postdepositional faulting and folding (Fig. 2B). Nevertheless, individual beds are well exposed and can be followed over several meters. A 3-cm-thick dark olive-green spherule-rich layer overlies an erosional surface separating Maastrichtian and Danian sediments (Figs. 2C and 2D). No major disturbances are recognized in the spherule-rich layer apart from syndepositional slumping and minor postdepositional faults that led to the layer triplication at one edge of the outcrop (Fig. 2E).

The light gray-yellow calcareous siliceous mudstones are mainly composed of planktic foraminifers, nannofossils, and radiolarians. These beds are typical pelagic deposits representing normal marine sedimentation (i.e., suspended material that was floating in the open ocean and has settled on the seafloor; Nichols, 2009).

The dark olive-brown litharenites are mainly composed of volcanic lithics (glass-rich) and plagioclase with calcite cement. Foraminifers, nannofossils, and radiolarians are also present. Common normal gradation and sorting (Figs. 2F and 2G), irregular bases (Fig. 2H), lack of upper-flow regime sedimentary structures, and grain size no larger than sand indicate deposition during the last stages of a typical turbidite at the distal end (i.e., deposition by waning flow energy and ultimately settling from suspension as the flow comes to rest; Bouma, 1962). A few beds in the late Maastrichtian show poorly sorted, structureless sediments above an erosional surface (Fig. 2I) interpreted as turbidite deposits with higher dynamic conditions (Bouma, 1962). Turbidites composed of volcanic material are very common in marine

environments proximal to volcanic provinces, such as Gorgonilla (Nichols, 2009).

The spherule-rich layer overlying the erosional surface has a clast-supported sedimentary fabric with normal gradation (Figs. 3A–3D). This litharenite contains abundant glass spherules, lithics (mostly volcanic; Figs. 3E–3H), and microfossils (Figs. 3I and 3J), and it transitions to a calcareous mudstone as particle size decreases (Fig. 3D). These characteristics are interpreted as deposition by waning turbidity flow, similar to the litharenites described above. An erosional base generally develops by the scouring action of the turbidity current on the usually finer deposits over which the current flows (Reineck and Singh, 1980). Turbidites also typically show a clast-supported sedimentary fabric as the coarser material transported by saltation and rolling is deposited while the finer material transported by suspension is washed away until dynamic conditions decrease (Reineck and Singh, 1980). Normal gradation refers to a distribution grading where coarse sediments (e.g., spherules, lithics, and larger-sized planktic foraminifera at Gorgonilla; Fig. 3B) progressively grade into finer sediments from the bottom to the top of a bed, and it can also be the result of deposition by turbidity currents (Reineck and Singh, 1980; Nichols, 2009).

Origin of the Gorgonilla Spherules

The Gorgonilla spherules are dark olive to light brown in color, mostly round (rarely oval, teardrop, and dumbbell morphologies), with a maximum diameter of 1.3 mm at the base of the layer (Figs. 3A–3C). Most of the spherules (70%–90%) consist of unaltered glass (massive or with vesicles infilled with calcite), and common alteration products include smectites, calcite, and zeolites (Bermúdez et al., 2016).

Glass spherules are formed through high-temperature processes associated with volcanic eruptions (e.g., Carracedo Sánchez et al., 2010; Walker and Croasdale, 1971) and meteorite impacts (e.g., Glass and Simonson, 2012; Smit, 1999). Volcanic spherules usually derive from lava fountains of low-viscosity basaltic magmas and are commonly found in ash deposits (e.g., Heiken, 1974; Melson et al., 1988; Vallier et al., 1977). When a large extraterrestrial body hits Earth, a plume of melted and vaporized rocks is ejected into the atmosphere, forming glass spherules upon cooling (solidified from melt, condensed from vapor). It then falls back to Earth's surface, where it may accumulate as a spherule layer (Glass and Simonson, 2012).

Because Gorgonilla Island sediments are rich in volcanic material, CO_2 laser ablation analysis of the oxygen isotope compositions of the glass spherules was used to test whether these spherules could be volcanic in origin. The $\delta^{18}O$ results of individual spherules showed a wide range of values from +8.5‰ to +10.4‰. Local basalt, if unaltered, is expected to have $\delta^{18}O$ values of about +6‰. However, if the glasses are somewhat altered, higher values are commonly measured for glasses of basaltic compositions (e.g., Eiler, 2001; Vennemann et al., 2001). If volcanic in origin, $\delta^{18}O$ values suggest a typical andesite-dacite (+8‰) rhyolitic glass (+9‰ to +10‰) composition. Hence the spherules could be (1) volcanic in origin with the glass altered during postdepositional processes (e.g., Vennemann et al., 2001), or (2) the result of volcanic melts contaminated by sedimentary material prior to eruption, or (3) impact melt ejecta of mixed basaltic-sedimentary material. The large range in values would, however, support either variable amounts of postdepositional alteration or variable proportions of basaltic-sedimentary material.

Major-element geochemistry showed that the Gorgonilla spherules are mainly composed of SiO_2 (46.43%–68.15%), Al_2O_3 (8.69%–15.85%), and CaO (5.45%–30.26%), with FeO (4.43%–5.85%), MgO (1.90%–4.84%), K_2O (0.28%–1.87%), Na_2O (0.97%–4.00%), and TiO_2 (0.42%–0.68%) as minor components (Fig. 4; Bermúdez et al., 2016). Comparing these results with the composition of known Chicxulub impact deposits, Gorgonilla spherules are similar to black and yellow (high-Ca) glass spherules found in Beloc, Haiti (Koeberl and Sigurdsson, 1992), and Mimbral, NE Mexico (Smit et al., 1992), thus confirming an impact origin. Some overlap is also observed with Fe-rich spherules at Demerara Rise, tropical western North Atlantic (Schulte et al., 2009), whereas K-rich spherules at Mimbral (Smit et al., 1992), smectite spherules at Demerara (Schulte et al., 2009), Fe- and K-rich spherules at La Sierrita, NE Mexico (Schulte et al., 2003), and smectite and chlorite spherules at Brazos River, Texas (Schulte et al., 2006), are very different (Fig. 4). These differences between Gorgonilla and some Chicxulub impact spherule deposits are associated with the degree of glass

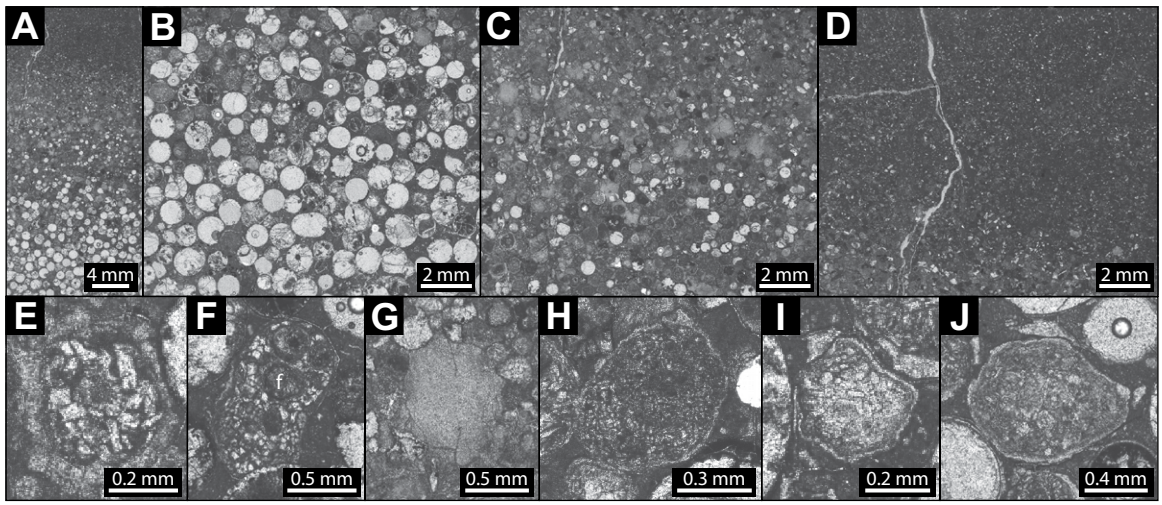

Figure 3. (A–J) Spherule-rich layer separating Maastrichtian and Danian sediments at the Gorgonilla section, Colombia. This deposit consists of a clast-supported, normally graded litharenite (A–D) with abundant glass spherules, lithics (mostly volcanic) (E–H), and microfossils (large Cretaceous planktic foraminifera) (I, J), which transitions to a calcareous mudstone as particle size decreases (D). These characteristics indicate deposition by waning turbidity flow. Glass spherules are mostly round (rarely oval, teardrop, and dumbbell morphologies), with a maximum diameter of 1.3 mm at the base of the layer (A–C). f—foraminifera.

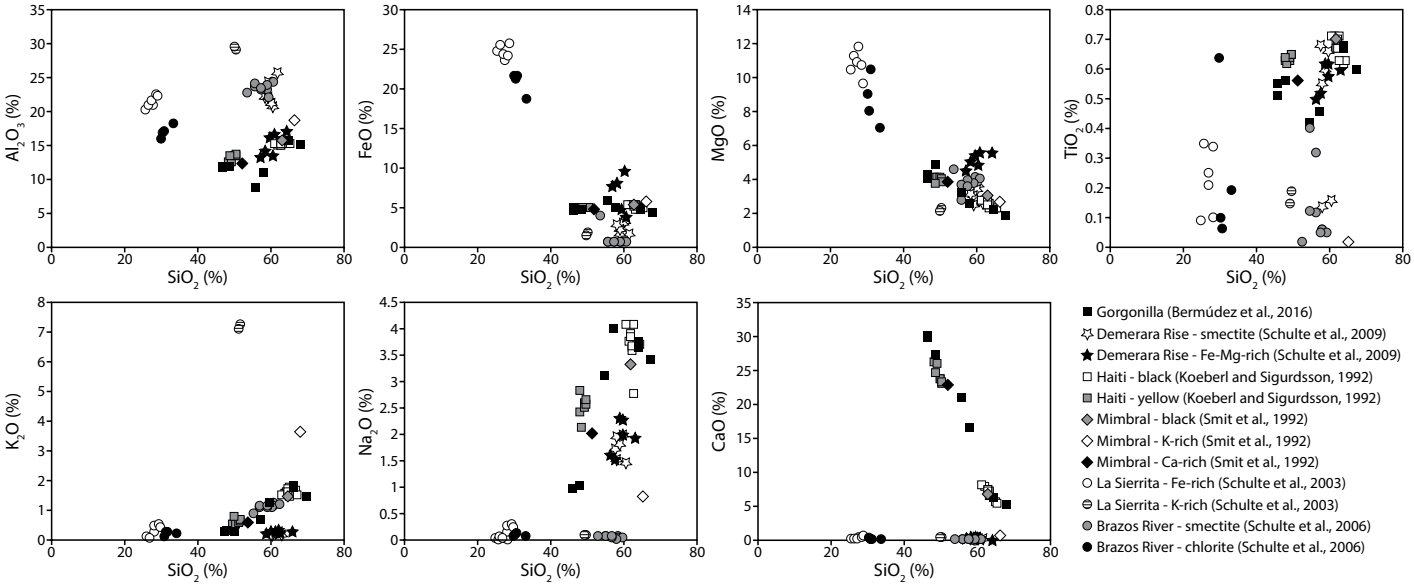

Figure 4. Major-elements composition of Gorgonilla glass spherules (Bermúdez et al., 2016) and comparison with Chicxulub impact spherules in NE Mexico (Mimbral—Smit et al., 1992; La Sierrita—Schulte et al., 2003), Texas (Brazos River—Schulte et al., 2006), Haiti (Koeberl and Sigurdsson, 1992), and tropical North Atlantic (Demerara Rise—Schulte et al., 2009). Gorgonilla spherules are similar to black and yellow (high-Ca) glass spherules found in Haiti and Mimbral, NE Mexico, thus confirming an impact origin. Differences with the other sites are associated with the degree of glass alteration.

alteration. At Gorgonilla, most of the spherules consist of unaltered glass. Haiti and Mimbral spherules are significantly weathered, but unaltered glass relicts are still present. In contrast, Demerara Rise, La Sierrita, and Brazos River spherules are almost totally replaced by smectite and chlorite, thus overprinting their original major-element composition.

Biostratigraphy

Planktic foraminifera and radiolarians are the most abundant microfossils in the Gorgonilla section. Planktic foraminiferal biostratigraphy is excellent for relative age dating and to assess the continuity of sediment deposition in Cretaceous-Paleogene boundary sections based on high-resolution age biozonation schemes for the Maastrichtian and Danian (Fig. 5; Keller et al., 1996, 2002b; Li and Keller, 1998). Radiolarian occurrences are rare in Cretaceous-Paleogene boundary sections worldwide, except in areas of upwelling such as New Zealand (Hollis, 1993, 1997, 2003) and Ecuador (Keller et al., 1997b). In New Zealand, radiolarians have been shown to have survived the Cretaceous-Paleogene boundary mass extinction, but significant faunal changes are apparent by a shift from nassellarian- to spumellarian-dominated assemblages (Hollis et al., 2003). The origin and evolution of two lineages of radiolarian species form the basis of the early Paleocene zonation (Fig. 5; Hollis, 1993, 1997).

Planktic Foraminifera

Planktic foraminifera are abundant in Gorgonilla but poorly preserved. Relative ages and hiatuses were assessed based on presence or absence of biozone index species and composition of the assemblages. The section records late Maastrichtian zones CF2 and CF1 and early Danian zone P1a(2), with a major hiatus at the Cretaceous-Paleogene boundary spanning part of zone CF1, all of zones P0 and P1a(1), and part of P1a(2).

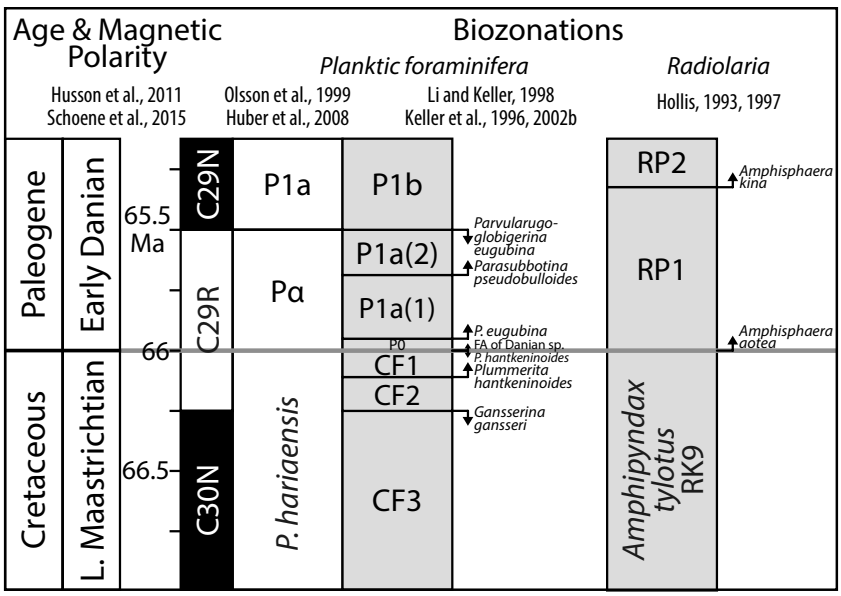

Figure 5. Late Maastrichtian to early Paleocene biostratigraphy for planktic foraminifera based on the zonation scheme of Li and Keller (1998) and Keller et al. (1996, 2002b) and for radiolaria based on Hollis (1993, 1997). Other zonal schemes are shown for comparison (Huber et al., 2008; Olsson et al., 1999). Magnetic polarity is from Husson et al. (2011), and radiometric ages are from Schoene et al. (2015). FA—first appearance.

Zone CF2 is defined by the last appearance (LA) of *Gansserina gansseri* at the base (base of magnetochron C29r) and first appearance (FA) of *Plummerita hantkeninoides* at the top, with an estimated duration of ~180 k.y.; zone CF1 spans the total range of the index species *P. hantkeninoides*, with an estimated duration of ~170 k.y. ending at the Cretaceous-Paleogene boundary (Fig. 5). These age estimates are based on current U-Pb dating of C29r (Schoene et al., 2015), a Cretaceous-Paleogene boundary age of 66.021 ± 0.024 Ma (Clyde et al., 2016), and sedimentation rates at Elles, Tunisia (Abramovich and Keller, 2002). At Gorgonilla, zone CF2 spans the first 2.13 m of the interval analyzed (Fig. 6). Large (>150 µm) globotruncanids and rugoglobigerinids were the only species identified in this interval. Zone CF1 spans from 11.13 m to 15.60 m just below the spherule-rich layer (Fig. 6). The planktic foraminiferal assemblage was diverse in the large size fraction (>150 µm) and consisted mainly of globotruncanids and rugoglobigerinids. The 63–150 µm and <63 µm size fractions were dominated by heterohelicids, small pseudoguembelinids, and hedbergellids. The presence of *P. hantkeninoides* below the spherule-rich layer was also reported in a preliminary biostratigraphic study of the Gorgonilla section, and rare small Danian species were interpreted as the result of burrowing (Bermúdez et al., 2016). In our subsequent field work, no burrowing structures were observed in the field, nor were early Danian species found below the spherule layer; the only small specimens present were Cretaceous hedbergellids.

At Gorgonilla, a hiatus (>250 k.y.) spans the Cretaceous-Paleogene boundary from the upper part of latest Maastrichtian zone CF1 through early Danian zones P0, P1a(1), and lower P1a(2) (Figs. 5 and 6). Similar erosion of the early Danian and topmost Maastrichtian spanning the Cretaceous-Paleogene boundary has been recorded worldwide (see section "How Complete is the Cretaceous-Paleogene Transition at Gorgonilla?"). In the earliest Danian, zone P0 defines the boundary clay and evolution of the first Danian species, including *Eoglobigerina edita*, *Parvularugoglobigerina extensa*, *Woodringina hornerstownensis*, and *Woodringina claytonensis*. Zone P1a spans the total range of *Parvularugoglobigerina eugubina*, ending at the magnetochron C29r/C29n boundary, and it can be subdivided into P1a(1) and P1a(2) based on the FA of *Parasubbotina pseudobulloides* and/or *Subbotina triloculinoides* (Fig. 5). At Gorgonilla, early Danian zone P0 and subzone P1a(1) are not present, marking a hiatus.

The first early Danian assemblage overlying the Cretaceous-Paleogene boundary hiatus is observed in the upper part (finer fraction) of the spherule-rich layer and sediments above, and it is typical of subzone P1a(2) (Fig. 6). This assemblage is diverse and includes the index species *P. eugubina*, *P. pseudobulloides*, and *S. triloculinoides*, in addition to *Chiloguembelina midwayensis*, *Chiloguembelina morsei*, *Eoglobigerina edita*, *Eoglobigerina eobulloides*, *Globoconusa daubjergensis*, *Guembelitria cretacea*, *Praemurica taurica*, *W. claytonensis*, and *W. hornerstownensis*. Similar assemblages in zone P1a(2) have been observed in North Atlantic and Tethys localities (Canudo et al., 1991; Keller, 1988; Keller and Abramovich, 2009; Keller and Benjamini, 1991; Keller et al., 2013; Mateo et al., 2016; Punekar et al., 2014b). Large

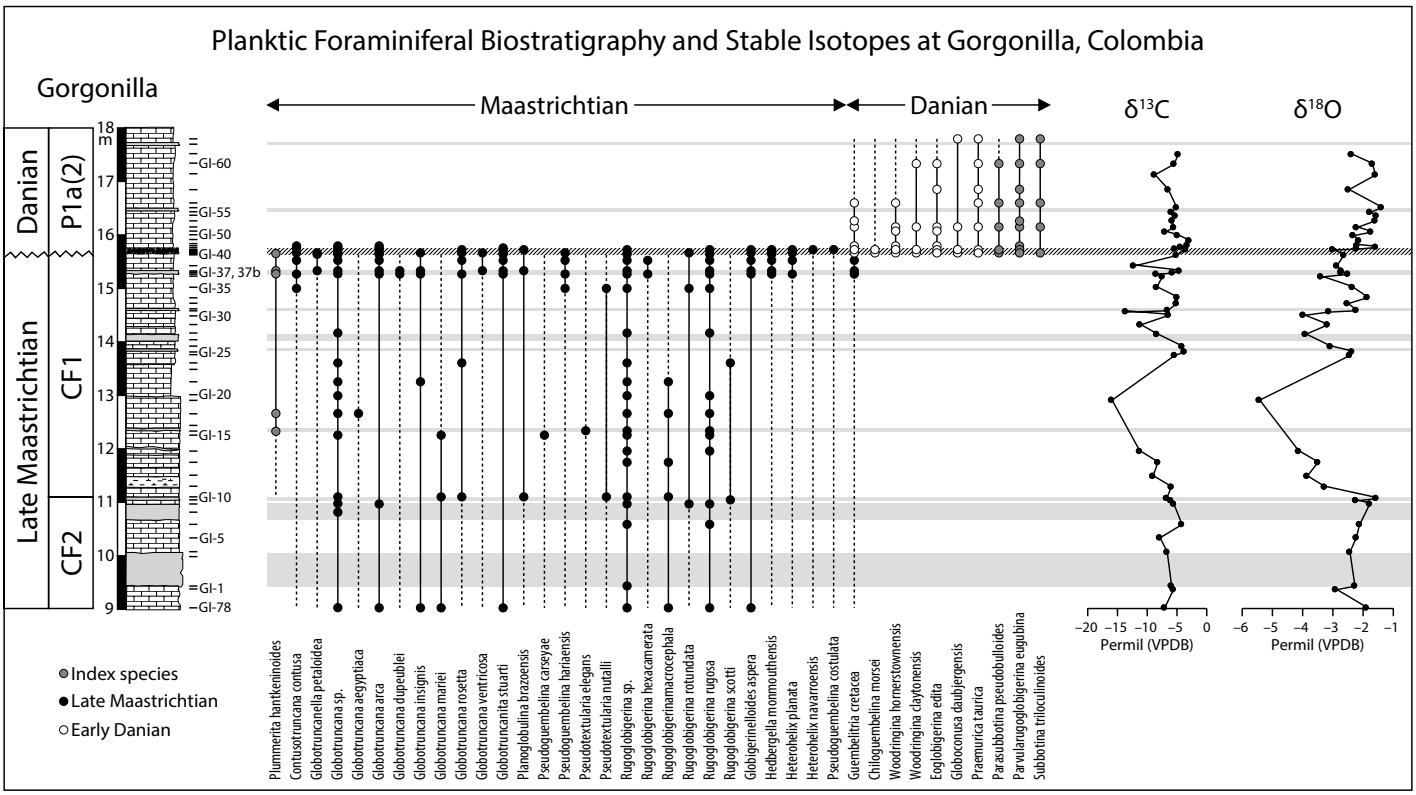

Figure 6. Planktic foraminiferal biostratigraphy and carbon and oxygen stable isotopes at the Gorgonilla section, Colombia. Gray bands mark turbiditic deposits. Striped band marks spherule-rich deposits. The section records late Maastrichtian zones CF2 and CF1 and early Danian zone P1a(2) with a major hiatus at the Cretaceous-Paleogene boundary spanning part of zone CF1, zone P0, zone P1a(1), and part of zone P1a(2). The absence of a negative shift in $\delta^{13}C$ at the Cretaceous-Paleogene transition, one of the five defining criteria used to identify the Cretaceous-Paleogene boundary, supports the Cretaceous-Paleogene boundary hiatus identified based on biostratigraphy. GI-# refers to each sample in our set. VPDB—Vienna Peedee belemnite.

Cretaceous species, mostly globotruncanids, are present just above the Cretaceous-Paleogene boundary hiatus, mostly concentrated at and near the base of the spherule-rich layer and mixed with spherules and lithics of similar size (Figs. 3I, 3J, and 6). In contrast, Danian species are found within large lithic clasts at the base of the spherule-rich layer and within fine sediments at the top, suggesting depositional processes that led to normal gradation (i.e., waning turbidity current and settling of turbidite material in suspension). Bermúdez et al. (2016) proposed that the presence of Danian species in the spherule layer might be the result of burrowing. However, the presence of microfossils in lithic clasts and fine sediments is not restricted to burrowing structures, which implies both older and/or contemporaneous deposition with the spherule-rich layer.

Radiolaria

Radiolarians are abundant and showed moderate to good preservation in both the calcareous siliceous mudstone and the turbiditic litharenites at Gorgonilla. Biostratigraphic interpretation of the assemblages is complicated by the occurrence of four distinct faunal elements (Fig. 7): (1) species that are known to range across the Cretaceous-Paleogene boundary, such as *Amphipyndax stocki*, *Dictyomitra andersoni* (Plate 1, no. 14, see footnote 1), and *Dictyomitra multicostata*; (2) species that are known from the latest Cretaceous in low latitudes and may well range in the Paleocene, such as *Amphipyndax tylotus* (Plate 1, no. 13, see footnote 1) and *Siphocampe altamontensis*; (3) rare species that are restricted to the Campanian, specifically *Amphipyndax pseudoconulus*, *Afens lirioides* (Plate 1, no. 7, see footnote 1), and *Theocampe urna*; and (4) equally rare species that have been thought to be restricted to the Paleocene. Although there are no obvious differences in preservation, our preliminary interpretation is that the Campanian elements were reworked into the late Maastrichtian–early Danian sediments. Assemblages spanning the Cretaceous-Paleogene boundary differ only in the rare occurrence of Paleocene-restricted spumellarians, notably *Amphisphaera kina* (Plate 1, nos. 2–3, see footnote 1) and *Amphisphaera goruna* (Plate 1, nos. 5–6, see footnote 1), in all samples examined above the spherule-rich layer (Fig. 7). The earliest Paleocene zone RP1 index species, *Amphisphaera aotea*, has not been observed in these samples, thus supporting a Cretaceous-Paleogene boundary hiatus. The absence of *A. aotea* could also imply that the *A. aotea–A. kina* succession was restricted to high latitudes. At odds with previous records, the Paleocene species *Buryella granulata* (Plate 1, 8–10, see footnote 1) occurred in two samples below the boundary, in addition to three of the Paleocene samples examined. This suggests that this species may have originated in low latitudes during the latest Cretaceous and migrated to higher latitudes in the early Paleocene. Apparent precursors to the Paleocene species *Lithostrobus longus* (Plate 1, 11–12, see footnote 1) were also present in Cretaceous and Paleocene samples. In summary, the overall similarities in assemblages from different lithologies (calcareous siliceous mudstones, turbiditic litharenites) below and above the Cretaceous-Paleogene boundary hiatus suggest that most of the radiolarians were discovered in place and signal survival of radiolarians across the boundary, as previously documented for Cretaceous-Paleogene boundary sections in the New Zealand region (Hollis, 1993, 1997). Further detailed census studies of these radiolarian-rich samples are required to confirm these preliminary observations.

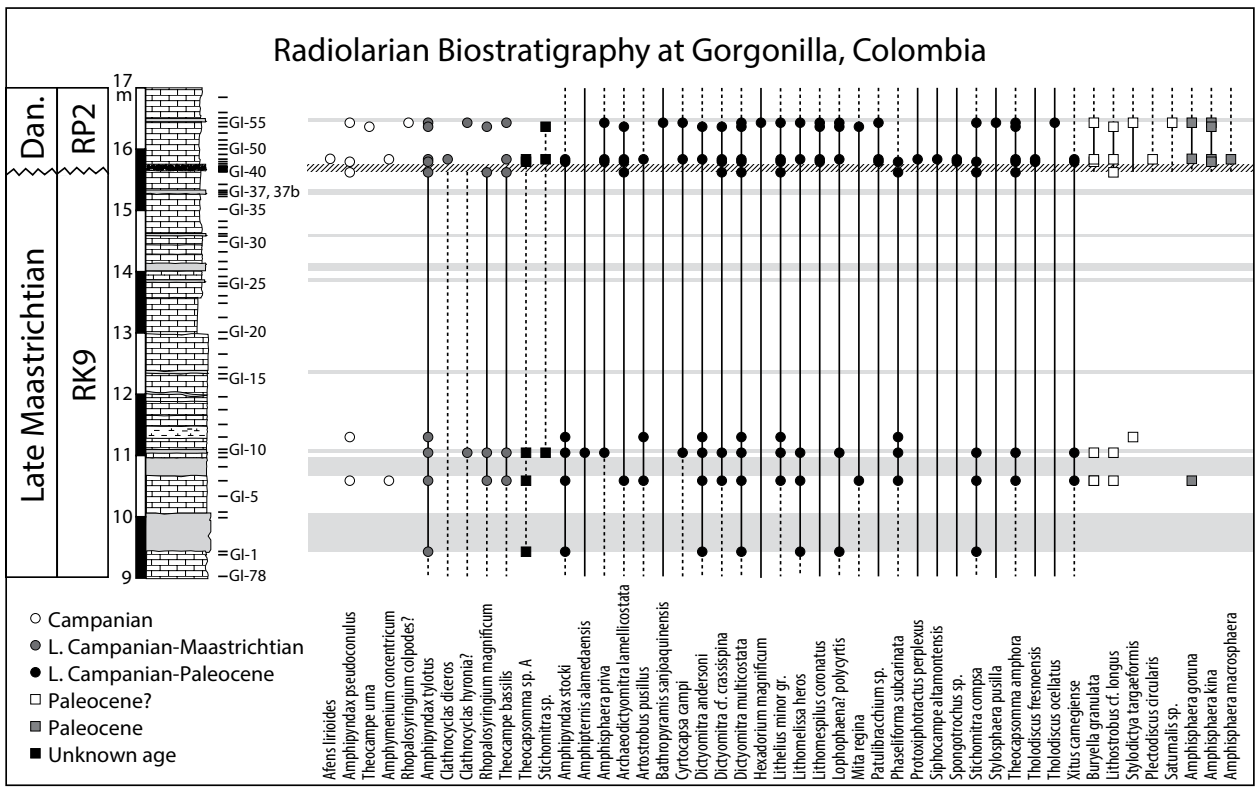

Figure 7. Radiolarian biostratigraphy at the Gorgonilla section, Colombia. Gray bands mark turbiditic deposits. Striped band marks spherule-rich deposits. A hiatus at the Cretaceous-Paleogene boundary is recorded by the absence of the earliest Paleocene zone RP1 index species *Amphisphaera aotea*, confirming findings based on planktic foraminiferal biostratigraphy and carbon stable isotopes. Representative species are shown in Plate 1 (see text footnote 1). GI-# refers to each sample in our set.

Carbon and Oxygen Stable Isotopes

Bulk-rock carbon and oxygen isotopes are used as proxies for productivity and climate, respectively. At Gorgonilla, diagenetic overprinting of the primary isotope signals is relatively minor, based on poor correlation coefficients between $\delta^{13}C$ and $\delta^{18}O$ (R^2 = 0.17), $\delta^{13}C$ and calcite (R^2 = 0.01), and $\delta^{18}O$ and calcite (R^2 = 0.001; Mitchell et al., 1997). Nonetheless, persistent local volcanism indicated by recurrent volcanic-rich turbidite deposits could have overprinted these isotopic records. Very low $\delta^{13}C$ values throughout the section suggest a significant source of ^{12}C, probably related to cracking of organic matter due to intense volcanic activity (typical organic matter $\delta^{13}C$ signal is –29‰, which is significantly lower than the $\delta^{13}C$ of ambient seawater, +1‰; Kump and Arthur, 1999).

At Gorgonilla, $\delta^{13}C$ values range from –7.9‰ to –4.2‰ (an average of –6.2‰), and $\delta^{18}O$ values range from –2.9‰ to –1.6‰ (an average of –2.2‰) in zone CF2 and rapidly decrease to an average of –10.1‰ and –4.1‰ above the CF2/CF1 boundary, respectively (Fig. 6). This decrease and following large fluctuations between –13.7‰ and –3.8‰ for $\delta^{13}C$ and between –4.0‰ and –1.9‰ for $\delta^{18}O$ in zone CF1 may be related to rapid global climate changes and environmental perturbations associated with the eruption of the Deccan Traps in India (e.g., Keller et al., 2016; Punekar et al., 2014a). Changes due to diagenetic alteration cannot be ruled out either.

One of the five defining criteria used to identify the Cretaceous-Paleogene boundary is a negative shift of 2‰–3‰ in $\delta^{13}C$ that represents the collapse in primary productivity during the Cretaceous-Paleogene boundary mass extinction (Keller, 2014). At Gorgonilla, the absence of this shift across the transition from Maastrichtian to Danian sediments confirms the Cretaceous-Paleogene boundary hiatus identified based on biostratigraphy (Fig. 6). Above the Cretaceous-Paleogene boundary hiatus, $\delta^{13}C$ and $\delta^{18}O$ values slightly increase to an average of –5.6‰ and –2.2‰, respectively, with no major fluctuations as expected for an early Danian zone P1a interval (e.g., Keller and Lindinger, 1989; Quillévéré et al., 2008; Stüben et al., 2002; Fig. 6).

Mineralogy

Relative changes in bulk-rock mineralogy generally indicate changes in sediment source, sea-level fluctuations, and intensity of weathering. At Gorgonilla, three discrete types of rock units are recognized: pelagic deposits, turbidites, and the spherule-rich layer. A comparison of the mineralogical composition of these units yielded insight into the depositional nature of the impact spherules.

The most abundant minerals in the Gorgonilla section are phyllosilicates, calcite, and Na-plagioclase, while quartz, feldspar, dolomite, pyrite, and goethite are minor components (Fig. 8). The unquantified component corresponds to poorly crystallized minerals (mainly opal with minor pyrite and goethite), pyroxenes (augite), and amphiboles. Maastrichtian and Danian pelagic deposits and turbidites were compared based on statistical mean differences. Results showed that pelagic deposits significantly changed their composition in the early Danian, whereas the turbidites composition remained statistically similar below and above the Cretaceous-Paleogene boundary hiatus. In addition, pelagic deposits and turbidites were also significantly different.

Maastrichtian pelagic deposits consisted primarily of calcite (32.0%), phyllosilicates (22.9%), unquantified minerals (mainly opal, pyroxenes, and amphibole, 19.4%), and Na-plagioclase (18.7%; Fig. 8; Table 1). In contrast, the most abundant mineral in Danian pelagic sediments were phyllosilicates (33.2%), followed by Na-plagioclase (26.0%), calcite (22.8%), and unquantified minerals (12.5%). This change from calcite-rich Maastrichtian deposits to phyllosilicate-rich Danian deposits probably reflects the reduction of calcium carbonate ($CaCO_3$) production in the aftermath of the Cretaceous-Paleogene boundary mass extinction (e.g., Caldeira and Rampino, 1993; Caldeira et al., 1990; Kump, 1991). Turbidites were dominated by phyllosilicates (45.8%), followed by Na-plagioclase (21.0%), unquantified minerals (15.1%), and calcite (10.6%; Fig. 8; Table 1). However, a few turbidite deposits showed higher calcite content, suggesting increased mixing with locally derived sediments due to higher dynamic conditions.

The main differences between pelagic deposits and turbidites were phyllosilicates and calcite contents, which are ultimately associated with different sediment sources. Pelagic sediments consist mostly of bioclastic materials (e.g., foraminifera, radiolaria) and other fine volcanic and terrigenous particles settling onto the seafloor (Nichols, 2009). In contrast, turbidites are typically the dominant clastic deposits in open-marine environments, resulting from turbidity currents that rework, transport, and redeposit material from shallower depths (with higher detrital content) into deeper waters (Nichols, 2009).

The most abundant minerals in the spherule-rich layer were phyllosilicates (46.4%) and calcite (36.5%; Fig. 8; Table 1). Because of the high phyllosilicates content, the spherule-rich layer is interpreted as another turbidite deposit, as also indicated by the lithology and biostratigraphy (note: only a small percentage of the phyllosilicates corresponds to spherule alteration products). The calcite content in the spherule-rich layer is largely due to infillings of spherule vesicles and shells of planktic foraminifera, especially large Cretaceous species reworked and transported downslope by the turbidity current.

DISCUSSION

How Complete Is the Cretaceous-Paleogene Transition at Gorgonilla?

As discussed above, biostratigraphy and stable isotopes show a major Cretaceous-Paleogene boundary hiatus at Gorgonilla that eliminates planktic foraminiferal zones P0 and P1a(1) and the Cretaceous-Paleogene boundary $\delta^{13}C$ negative shift that marks the mass extinction and also truncates part of zones CF1 and P1a(2) (Fig. 6). The missing interval is estimated at >250 k.y. (based on current U-Pb dating of C29r [Schoene et al., 2015], the age of 66.021 ± 0.024 Ma for the Cretaceous-Paleogene boundary [Clyde et al., 2016], and sedimentation rates at Elles, Tunisia [Abramovich and Keller, 2002]). Trace-element analysis on the matrix of the spherule-rich layer showed the absence of significant Ni, Co, and Cr enrichments, characteristic of Cretaceous-Paleogene boundary deposits, therefore supporting the presence of a Cretaceous-Paleogene boundary hiatus (T. Adatte and A. Bitchong, 2017, personal commun.). The Cretaceous-Paleogene transition at Gorgonilla is thus incomplete, with the critical Cretaceous-Paleogene boundary event missing.

In contrast, Renne et al. (2018) reported a Cretaceous-Paleogene boundary hiatus at Gorgonilla that spanned no more than 10 k.y., based on the presence of a bloom in the planktic foraminiferal species *Guembelitria cretacea* interpreted as the Planktic Foraminiferal Acme Stage 1 (PFAS-1) of Arenillas et al. (2006), which occurred right after the Cretaceous-Paleogene boundary. However, this is a poor basis for age control because *Guembelitria cretacea* is the only long-term survivor of the end-Cretaceous mass extinction, with blooms reported from the late Maastrichtian into early Paleocene zone P1b more than 500 k.y. after the Cretaceous-Paleogene boundary (e.g., Keller and Benjamini, 1991; Pardo et al., 1996; Abramovich et al., 1998, 2010, 2011; Keller, 1988, 1989, 2001, 2002; Keller et al., 1996, 2011a, 2011b, 2012, 2013; Canudo et al., 1991; MacLeod and Keller, 1994; Molina et al., 1998; Luciani, 2002; Pardo and Keller, 2008; Punekar et al., 2014a, 2014b). Clearly, a *Guembelitria* bloom above the spherule-rich

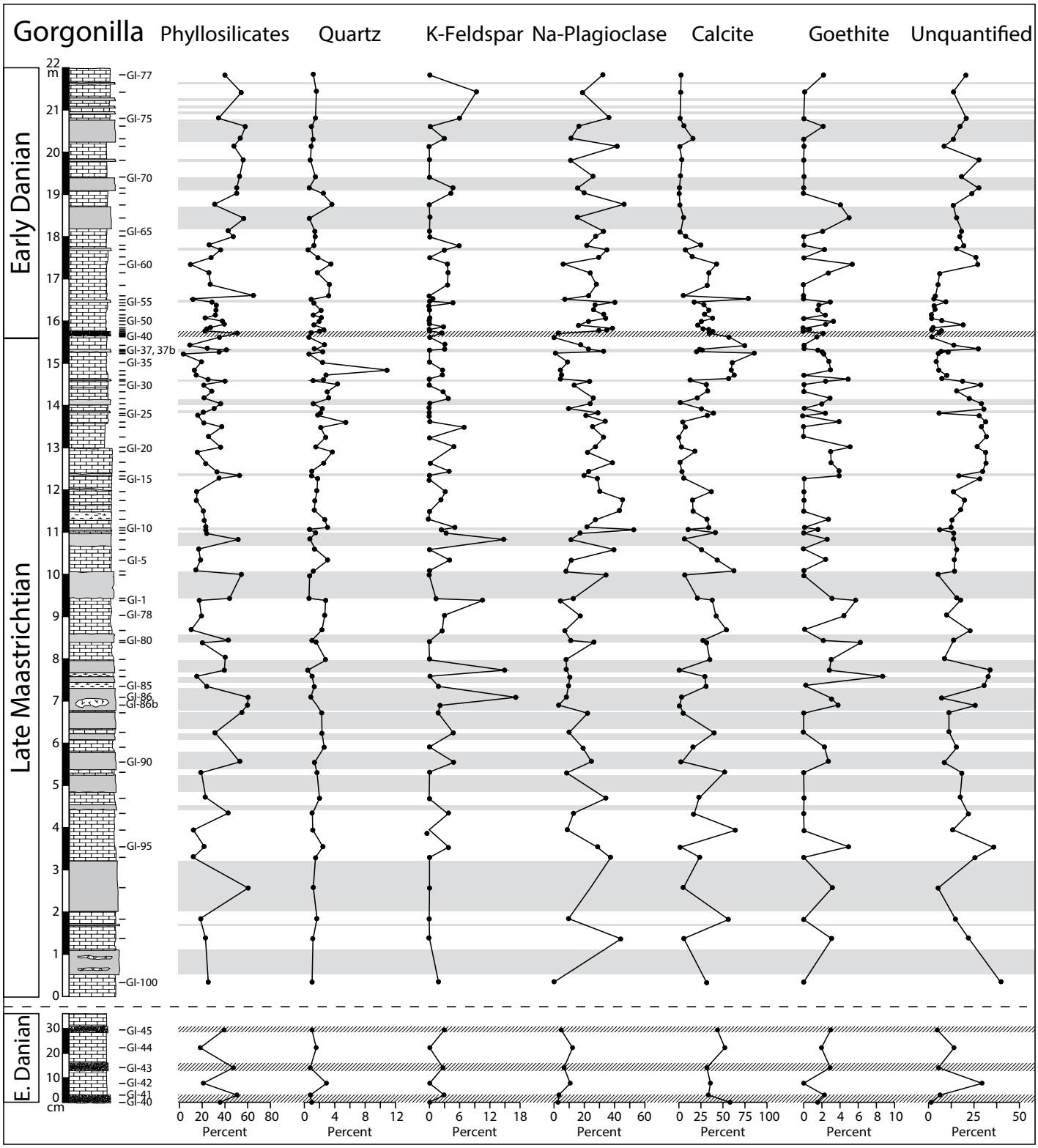

Figure 8. Bulk-rock mineralogy at the Gorgonilla section, Colombia. Unquantified minerals refer to opal, pyroxene, and amphibole (not quantified due to the low intensity of their respective peaks and/or absence of good representative standards). Gray bands mark turbiditic deposits. Striped bands mark spherule-rich deposits (note that the three striped bands represent the same spherule layer that was triplicated at one edge of the outcrop by syndepositional slumping and minor postdepositional faulting). The most abundant minerals in the spherule-rich layer are phyllosilicates, similar to the turbiditic deposits. GI-# refers to each sample in our set.

TABLE 1. BULK-ROCK MINERALOGY AT THE GORGONILLA SECTION, COLOMBIA

	Phyllosilicates (%)	Quartz (%)	K-feldspar (%)	Na-plagioclase (%)	Calcite (%)	Dolomite (%)	Pyrite (%)	Goethite (%)	Unquantified (%)
Pelagic sediments (Maastrichtian)									
Avg	22.93	2.25	1.67	18.70	32.01	0.38	0.92	1.62	19.44
SD	9.94	1.59	2.29	12.75	21.34	0.67	0.69	2.18	9.37
n	49	49	49	49	49	49	49	49	49
lower	20.08	1.80	1.02	15.04	25.88	0.19	0.72	1.00	16.75
upper	25.79	2.71	2.33	22.36	38.14	0.58	1.12	2.25	22.13
Pelagic sediments (Danian)									
Avg	33.15	1.91	1.66	25.94	22.82	0.18	0.75	1.10	12.48
SD	13.62	0.81	2.58	10.07	19.53	0.34	0.74	1.48	8.97
n	27	27	27	27	27	27	27	27	27
lower	27.76	1.59	0.64	21.96	15.09	0.04	0.46	0.51	8.94
upper	38.54	2.23	2.68	29.93	30.55	0.31	1.05	1.68	16.03
Turbidites									
Avg	45.84	1.04	3.12	21.03	10.58	0.33	0.74	2.24	15.07
SD	11.91	0.52	5.19	12.16	10.18	0.55	0.70	1.29	8.56
n	23	23	23	23	23	23	23	23	23
lower	40.69	0.82	0.88	15.77	6.18	0.09	0.44	1.68	11.37
upper	50.99	1.27	5.37	26.28	14.98	0.57	1.04	2.80	18.78
Spherule-rich layer									
Avg	46.40	0.80	2.74	4.09	36.48	0.63	1.04	2.59	5.23

Note: Unquantified minerals refer to opal, pyroxene, and amphibole (not quantified due to the low intensity of their respective peaks and/or absence of good representative standards). Avg—average, SD—standard deviation, *n*—number of samples, lower—lower bound of the 95% confidence interval, upper—upper bound of the 95% confidence interval.

layer at Gorgonilla cannot be used to age date the duration of the Cretaceous-Paleogene boundary hiatus. Moreover, Renne et al. (2018) only focused on the time missing above the boundary (which they estimated at 10 k.y.), but the missing zones P0 and P1a(1) span about half of C29r above the Cretaceous-Paleogene boundary (~250 k.y.). They also ignored the potentially missing interval of the Maastrichtian below the boundary, even though they claimed there is no evidence of zone CF1 index species *P. hantkeninoides*, which would lead to a missing Maastrichtian interval of ~170 k.y.

Erosion across the Cretaceous-Paleogene boundary is common and has been recorded worldwide, where a hiatus frequently spans from the late Maastrichtian zones CF2 or CF3 through most or all of early Danian zones P1a(1) and P1a(2) or P1b (Fig. 9). In more complete sections, like Gorgonilla, a shorter Cretaceous-Paleogene boundary hiatus is also present spanning part or all of zone CF1, zone P0, and part or all of P1a(1). Local conditions (e.g., current intensity, rate of sedimentation) usually affect the extent of erosion, with the more complete sequences only showing short intrazone hiatuses (Fig. 9). The Cretaceous-Paleogene boundary erosion is commonly attributed to rapid climate changes, enhanced bottom-water circulation during global cooling, sea-level fluctuations, and/or intensified tectonic activity (e.g., Keller et al., 2013; MacLeod and Keller, 1991; Mateo et al., 2016). At Gorgonilla, intense and persistent volcanism during the late Maastrichtian to early Danian, indicated by the large amount of volcanic material in turbidite deposits, likely contributed to the Cretaceous-Paleogene boundary erosion.

Age and Nature of the Gorgonilla Spherule-Rich Layer

The stratigraphic position of Chicxulub impact deposits, such as the spherule-rich layer at Gorgonilla, is a key factor for interpreting the age of this impact relative to the Cretaceous-Paleogene boundary mass extinction. Only primary spherule deposits representing direct fallout from the impact with no subsequent reworking can yield this information. Unfortunately, most Chicxulub impact spherule layers are reworked and redeposited into younger sediments and therefore provide no stratigraphic evidence from which the timing of the impact can be inferred (e.g., Keller et al., 2013; Mateo et al., 2016). Indeed, claims of ultimate proof that the impact is Cretaceous-Paleogene boundary in age based on spherule layers at the boundary have generally failed to recognize the reworked nature of these spherule deposits, including early Danian fauna that evolved long after the mass extinction and a hiatus (e.g., Norris et al., 1999, 2000; Olsson et al., 1997; Schulte et al., 2009; see also Figs. 9 and 10 herein). It is thus imperative to assess the depositional nature of spherule deposits before drawing any conclusions regarding the timing of the Chicxulub impact.

Relative Age of the Gorgonilla Spherule-Rich Layer

Biostratigraphy at Gorgonilla shows that sediments below the spherule-rich layer were deposited during the late Maastrichtian planktic foraminiferal zone CF1, and sediments above the spherule-rich layer were deposited during Danian zone P1a(2) (Fig. 6). Within the spherule-rich layer, both Maastrichtian and Danian species are present, indicating a mixture of sediments from different ages (Fig. 6). The youngest species are characteristic of zone P1a(2), with the same assemblages in the pelagic sediments above the spherule layer. Therefore, the depositional age of this spherule-rich layer is zone P1a(2), at least 250–300 k.y. after the Cretaceous-Paleogene boundary. Bermúdez et al. (2016) argued that the spherule-rich layer represents primary fallout from Chicxulub at Cretaceous-Paleogene boundary time and that absence of Danian microfossils at the very base cannot falsify this interpretation. The main problem with this interpretation is that the spherule-rich layer is a single turbiditic event and consequently shows no breaks in sedimentation, as we would expect if the age of the spherules at the very base were different from the age of spherules in the upper part of this 3-cm-thick layer (Fig. 3A). Therefore, if sediments at the top correspond to zone P1a(2), then deposition of spherules at the base must correspond to zone P1a(2). The distribution of large spherules and Cretaceous foraminifera at the base and small Danian foraminifera at the top of the spherule-rich layer represent normal gradation that resulted from settling of larger and heavier particles followed by successively smaller and lighter particles, which included the very small early Danian species.

Depositional Nature of the Gorgonilla Spherule-Rich Layer

The Gorgonilla spherule-rich layer was previously interpreted as an undisturbed deposit representing primary fallout and settling through

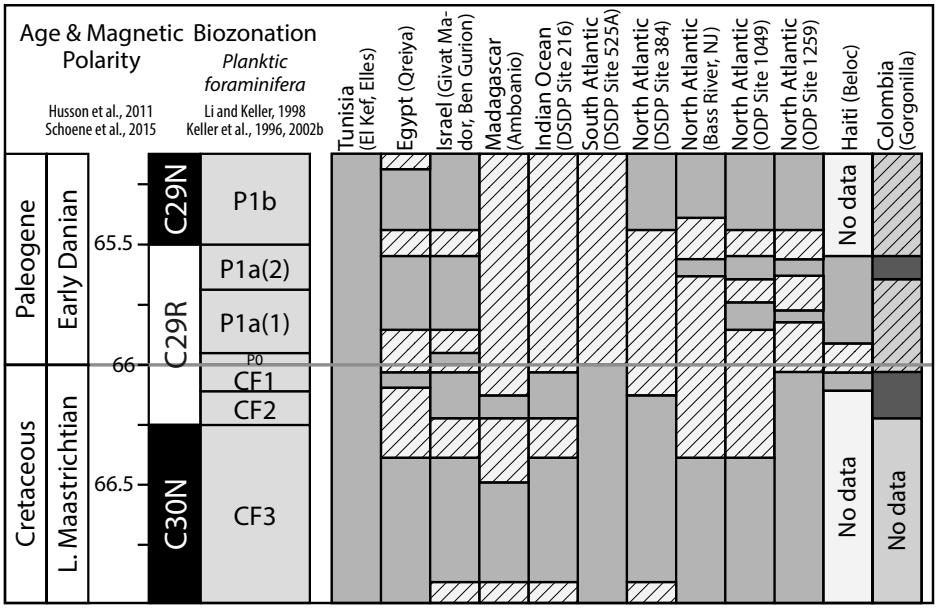

Figure 9. Overall correlation of hiatuses during the Cretaceous-Paleogene transition reflecting increased climate variability, intensified currents, and erosion on a global scale: Qreiya, Egypt (Punekar et al., 2014b); Givat Mador and Ben Gurion, Israel (Keller and Benjamini, 1991); Amboanio, Madagascar (Abramovich et al., 2003); Deep Sea Drilling Project (DSDP) Site 216, Indian Ocean (Keller et al., 2016); DSDP Site 525A, South Atlantic (Abramovich and Keller, 2003; Li and Keller, 1998); DSDP Site 384, North Atlantic (Mateo et al., 2016); Bass River, New Jersey, Ocean Drilling Program (ODP) Site 1049 and ODP Site 1259, North Atlantic (Keller et al., 2013); Beloc, Haiti (Keller et al., 2001); Gorgonilla, Colombia (this study). El Kef and Elles sections, Tunisia, are considered to be the most complete Cretaceous-Paleogene boundary sections in the world (Keller, 1988; Keller and Lindinger, 1989; Keller et al., 2002b) and are shown for comparison.

the water column of Chicxulub impact spherules followed by current activity (Bermúdez et al., 2016). This interpretation was based on the near absence of biogenic and detrital material between spherules at the very base (i.e., settling through the water column) and an increase in the amount of mixed material toward the top of the layer (i.e., current activity). In contrast, our study reveals that spherule deposition occurred via turbidity currents similar to repeated turbidite deposits throughout the section (see the "Lithology" subsection of the "Results"). Bermúdez et al. (2016) failed to address at least five key points in their alternative interpretation. (1) They argued that deposition of the spherule-rich layer was the result of two different depositional processes: first, primary settling from suspension followed by current activity disturbing the upper part of the spherule layer. If this were the case, then there should be a break in sedimentation, but there is none, as previously discussed ("Lithology" subsection; Fig. 3A). (2) If spherule deposition were the result of primary settling from suspension, normal gradation should only affect the spherule size distribution, because normal marine sedimentation randomly accumulates material on the seafloor without particular sorting (i.e., no gradation). At Gorgonilla, spherules, lithics, and microfossils are all normally graded from the very base to the very top of the spherule-rich layer (Figs. 3A–3D), indicating that the entire layer, including reworked Cretaceous microfossils, was the result of the same depositional process. (3) Graded bedding directly associated with settling of suspended material can only be observed in shallow-water environments, where dispersion and mixing are minor. In contrast, most graded beds in deep-water environments, such as the lower bathyal slope at Gorgonilla, are the result of turbidity currents (Nichols, 2009). (4) The age of the spherule-rich layer corresponds to early Danian zone P1a(2), at least 250–300 k.y. after the Cretaceous-Paleogene boundary, and therefore it does not represent the presumed Cretaceous-Paleogene boundary age of the Chicxulub impact (Fig. 6). It should also be noted that a Cretaceous-Paleogene boundary age for the Chicxulub impact is based on the assumption that this impact was Cretaceous-Paleogene boundary in age (reviews in Schulte et al., 2010; Keller, 2011). However, impact spherules are abundant near the base of zone CF1 in late Maastrichtian sediments throughout NE Mexico and Texas, and zone CF1 sediments overlie impact breccia in the Chicxulub impact crater core (review in Keller, 2012). (5) Bermúdez et al. (2016) argued that the presence of concave-convex contacts and agglutinated spherules indicates settling while still hot and therefore supports their interpretation that the Gorgonilla spherules represent a primary deposit. This argument has several flaws: (a) A majority of the spherules are perfectly spherical, (b) rare concave-convex contacts and amalgamated spherules are poorly developed compared with such features in the primary deposits of NE Mexico (see next section; Fig. 3A; Keller et al., 2009a), and (c) such rare occurrences can be explained as reworked material from a primary deposit and/or the result of postdepositional compaction.

Comparison with Other Chicxulub Impact Spherule-Rich Deposits

Since the discovery of the Chicxulub impact structure in the Yucatan Peninsula (Hildebrand et al., 1991; Pope et al., 1991), many impact spherule-rich deposits, both primary and reworked, have been documented at or near the Cretaceous-Paleogene boundary in the Gulf of Mexico (e.g., Alvarez et al., 1992; Keller et al., 1994a, 2009a; Lopez-Oliva and Keller, 1996; Schulte et al., 2003; Smit, 1999; Smit et al., 1992, 1996; Stinnesbeck et al., 1993), Texas (e.g., Adatte et al., 2011; Keller et al., 2007, 2011b; Schulte et al., 2006; Yancey, 1996), Caribbean Sea, Haiti, Belize, and Guatemala (e.g., Izett et al., 1990; Maurrasse and Sen, 1991; Sigurdsson et al., 1991; Smit et al., 1996; Stinnesbeck et al., 1997; Keller et al., 2001, 2003b; Alegret et al., 2005), and the North Atlantic Ocean (e.g., Olsson et al., 1997; Norris et al., 1999; MacLeod et al., 2007; Keller et al., 2013; Fig. 10).

Primary spherule deposits marking direct fallout from the Chicxulub impact are best known from El Peñon, NE Mexico (Keller et al., 2009a). A 2-m-thick spherule-rich unit was discovered in late Maastrichtian zone CF1 sediments deposited in an upper bathyal slope environment (Keller et al., 2009a). The basal part of this spherule unit consists of densely packed glass shards, compressed and welded spherules, 2–5 mm in diameter, with common concave-convex contacts (Fig. 11). Interstitial spaces are infilled with calcite and devoid of detrital or biogenic material. This suggests rapid deposition of still-hot impact glass that possibly accumulated as rafts on the sea surface before rapidly sinking to the seafloor (Keller et al., 2009a). Toward the top, spherules decrease in abundance and size and are generally isolated in a marly matrix

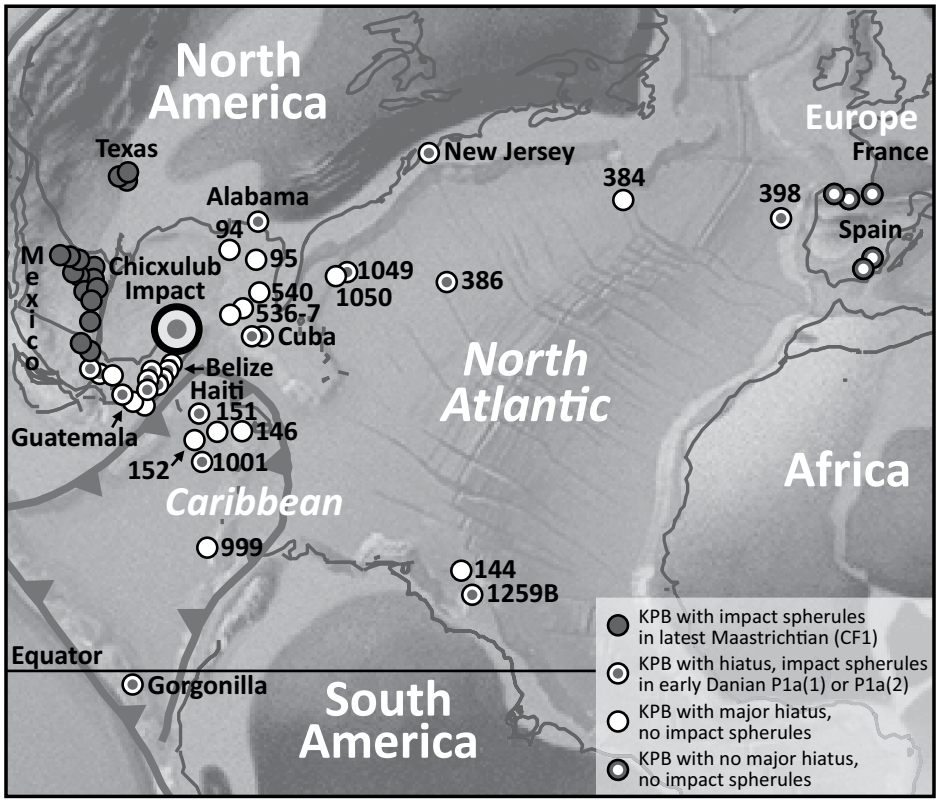

Figure 10. Paleogeography at the Cretaceous-Paleogene (KPB) transition and paleolocations of Cretaceous-Paleogene boundary sections previously analyzed. Paleolocation symbols indicate presence or absence of Chicxulub impact spherules and their stratigraphic age. Only NE Mexico and Texas record impact spherule layer within late Maastrichtian zone CF1 (~170 k.y. before the Cretaceous-Paleogene boundary), while impact spherules in all other localities (Gulf of Mexico, Caribbean, and North Atlantic) are reworked into early Danian zone P1a(1) or P1a(2) (~100 k.y. after the Cretaceous-Paleogene boundary) overlying hiatuses of variable extent. Impact spherules at Gorgonilla represent a reworked deposit within early Danian zone P1a(2) sediments. Figure is modified from Mateo et al. (2016).

with the same mineralogical composition as the overlying pelagic deposits, which indicates that current activity affected the top of the deposit sometime after settling (Fig. 12; Keller et al., 2009a).

The Gorgonilla spherule-rich layer shows none of the characteristic melted glass features of those from NE Mexico. Instead, deposition occurred in the early Danian zone P1a(2), impact spherules are primarily spherical with no evidence of compression or welding (Fig. 13), volcanic lithics and planktic foraminifera are common (Fig. 3), the matrix is detrital, and the mineralogical composition is significantly different from the overlying pelagic sediments (Fig. 8; Table 1).

Reworked Chicxulub impact spherules are ubiquitous, associated with intense erosion, transport, and redeposition of late Maastrichtian sediments due to sea-level changes and intensification of the Gulf Stream, mostly affecting Caribbean and North Atlantic sites (e.g., Keller et al., 2013). One of the first Chicxulub spherule-rich deposits was found in Beloc, Haiti (e.g., Izett, 1991; Izett et al., 1990; Sigurdsson et al., 1991). Even though this deposit was initially thought to be primary and coincident with the Cretaceous-Paleogene boundary (e.g., Izett, 1991; Izett et al., 1990, 1991; Lamolda et al., 1997; Maurrasse and Sen, 1991; Sigurdsson et al., 1991; Van Fossen et al., 1995), high-resolution biostratigraphic studies show that it had been reworked into the early Danian zone P1a(1) above a Cretaceous-Paleogene boundary hiatus (Keller et al., 2001). This spherule-rich deposit overlies late Maastrichtian zone CF1 sediments above an erosional surface with subrounded clasts of limestone, mudstone, and wackestone. The most expanded section shows a 70-cm-thick spherule-rich deposit represented by alternating layers with different abundances of spherules, and detrital and biogenic material. These layers are normally graded and show erosional contacts and were interpreted as the result of discrete turbiditic events (Fig. 14; Keller et al., 2001). Spherules reach a maximum diameter of 3.5 mm and are mostly altered to calcite and smectite, even though some black glass spherules with altered rims and yellow, vesicular glass spherules are also observed (Izett et al., 1990; Keller et al., 2001). Late Maastrichtian and early Danian planktic foraminiferal species are commonly present and mixed within the spherule-rich deposit (Keller et al., 2001).

The spherule-rich layer at Gorgonilla reveals very similar characteristics to Haiti, including a normally graded deposit above an erosional surface (Figs. 2C, 2D, and 3A) and late Maastrichtian and early Danian planktic foraminifera mixed with lithic clasts and spherules in a detrital matrix (Figs. 3 and 6). At Haiti, the thicker deposit with larger spherules can be explained by proximity to the Chicxulub impact site (~800 km), in comparison to the more distant Gorgonilla locality (~3000 km).

Ocean Drilling Program (ODP) Site 1259B on Demerara Rise, off the coast of Venezuela, is another example of a reworked spherule deposit that was initially interpreted as primary Chicxulub impact ejecta (MacLeod et al., 2007; Schulte et al., 2009). A 2-cm-thick spherule-rich layer with normal gradation is observed above an erosional contact marking a Cretaceous-Paleogene boundary hiatus (Fig. 15; Keller et al., 2013). Sediments below the spherule-rich layer correspond to the late Maastrichtian zone CF1, and sediments above are early Danian zone P1a(1). The spherule-rich layer shows both late Maastrichtian and early Danian species along with detrital material presumably from erosion and transport from the Guyana craton (Keller et al., 2013). The Gorgonilla spherule-rich layer is comparable with the reworked impact deposit at Demerara Rise, thus further supporting deposition by turbidity currents long after the Chicxulub impact.

Age of the Chicxulub Impact

The age of the Chicxulub impact has been controversial since the discovery of the impact site in the Yucatan Peninsula. Impact spherules found in the Gulf of Mexico, Caribbean, and North Atlantic have been used to assess the age of the impact based on their stratigraphic position relative to the mass extinction horizon.

The stratigraphically oldest spherule-rich deposits have been found in NE Mexico and Texas near the base of late Maastrichtian zone CF1, predating the Cretaceous-Paleogene boundary by ~170 k.y. (Keller et al., 2002a, 2009a, 2009b). Subsequent erosion and redeposition

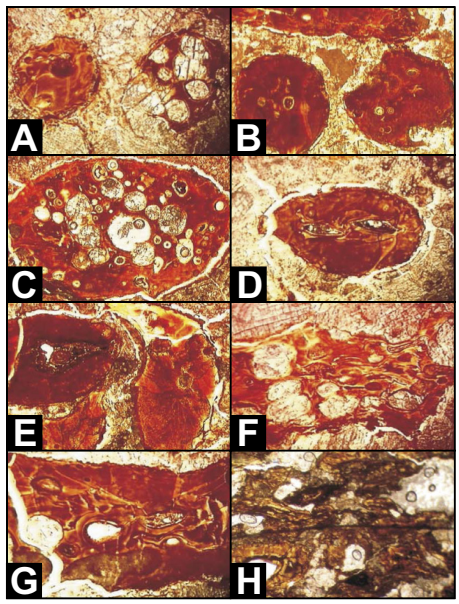

Figure 11. (A–H) Primary spherule deposit at El Peñon, NE Mexico, marking direct fallout from the Chicxulub impact. Deposition occurred rapidly, possibly by raft-like accumulation of hot spherules at the sea surface and rapid sinking. The basal part of this spherule unit is devoid of detrital or biogenic material and consists of vesicular spherules (A, B), compressed spherules (C, D) with common concave-convex contacts (E), glass shards (F, G), and welded, amalgamated spherules (H). Pictures are from Keller et al. (2009a). Spherules range from 2 mm to 5 mm in size.

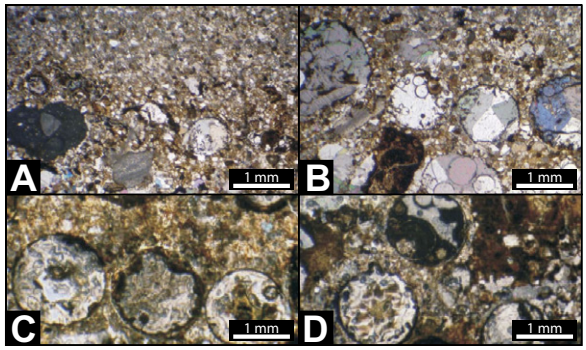

Figure 12. (A–D) Primary spherule deposit at El Peñon, NE Mexico, marking direct fallout from the Chicxulub impact. Toward the top of this unit, spherules decrease in abundance and size and are generally isolated in a marly matrix, suggesting that current activity affected the top of the deposit sometime after settling. Pictures are from Keller et al. (2009a).

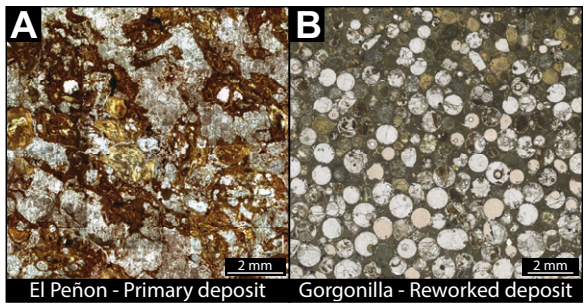

Figure 13. Comparison between (A) primary Chicxulub impact spherules at El Peñon, NE Mexico (Keller et al., 2009a), and (B) reworked Chicxulub impact spherules at Gorgonilla, Colombia. The Gorgonilla deposit shows none of the characteristic melted glass features of NE Mexico. Instead, impact spherules are primarily spherical with no evidence of compression or welding, volcanic lithics and planktic foraminifera are common, and the matrix is detrital.

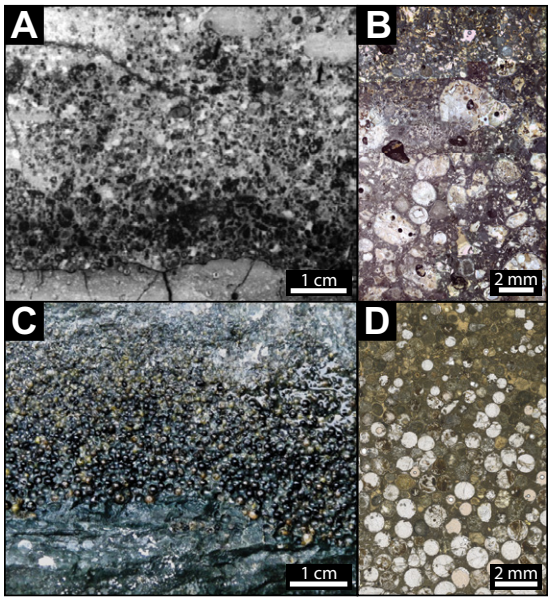

Figure 14. Comparison between (A, B) reworked Chicxulub impact spherules in Haiti (Izett, 1991; Keller et al., 2001) and (C, D) reworked Chicxulub impact spherules at Gorgonilla, Colombia. Both deposits overlie an erosional surface, are normally graded, and show a mix of spherules, lithics, and Maastrichtian and Danian microfossils in a detrital matrix, indicating deposition by turbiditic events. (Photo credit for C: Hermann Bermúdez.)

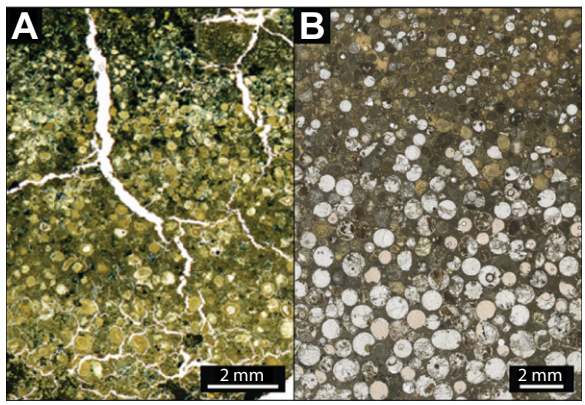

Figure 15. Comparison between (A) reworked Chicxulub impact spherules at Ocean Drilling Program (ODP) Site 1259, tropical North Atlantic (Keller et al., 2013; Schulte et al., 2009) and (B) reworked Chicxulub impact spherules at Gorgonilla, Colombia. Both deposits consist of a thin, normally graded, spherule-rich layer with abundant lithics and Maastrichtian and Danian microfossils above an erosional contact, indicating deposition by turbidity currents long after the Chicxulub impact.

of these primary deposits left multiple reworked spherule-rich layers within zone CF1 (Fig. 10) at the base of submarine channels filled with sandstones and marls below the Cretaceous-Paleogene boundary (Adatte et al., 1996, 2011; Keller, 2007; Keller et al., 2002a, 2003a, 2004a, 2004b, 2007, 2009a, 2009b; Stinnesbeck et al., 1993, 1996). Alternatively, these reworked spherules have been interpreted as the primary fallout of the Chicxulub impact followed by impact-induced tsunami deposits at the Cretaceous-Paleogene boundary, thus reconciling the stratigraphic separation of spherules and the Cretaceous-Paleogene boundary as due to the same impact event (e.g., Heymann et al., 1998; Schulte et al., 2006; Smit, 1999; Smit et al., 1992, 1996), while the oldest, actually primary spherule-rich deposits were interpreted as slumps (Schulte et al., 2003, 2010; Soria et al., 2001). However, evidence of bioturbation as well as discrete volcanic ash layers within sediments in between impact spherules and the Cretaceous-Paleogene boundary indicate normal marine sedimentation over tens of thousands of years, strongly suggesting that the impact preceded the mass extinction (Adatte et al., 1996; Ekdale and Stinnesbeck, 1998; Keller et al., 1994b, 1997a, 2007; Stinnesbeck et al., 1993, 1996).

In the Caribbean and North Atlantic, impact spherules in between Maastrichtian and Danian sediments (with no controversial tsunami deposits) have been interpreted as the ultimate proof that the Chicxulub impact occurred at the Cretaceous-Paleogene boundary and caused the mass extinction (e.g., Izett et al., 1990; Maurrasse and Sen, 1991; Norris et al., 1999; Olsson et al., 1997; Sigurdsson et al., 1991; Smit et al., 1992, 1996; Smit, 1999; Schulte et al., 2009). However, high-resolution planktic foraminiferal biostratigraphy has shown that most of these deposits have been reworked within early Danian zone P1a(1) and/or P1a(2) above a major Cretaceous-Paleogene boundary hiatus spanning from late Maastrichtian zone CF1 (and frequently CF2 and CF3) to the early Danian (e.g., Keller, 2007; Keller et al., 2001, 2003b, 2013; Mateo et al., 2016; Fig. 10).

Can radiometric dating ($^{40}Ar/^{39}Ar$) solve this controversy over the age of the Chicxulub impact? Since the early 1990s, radiometric dating has been the preferred solution to solve this argument. Early $^{40}Ar/^{39}Ar$ dating of impact spherules yielded ages supposedly synchronous with the Cretaceous-Paleogene boundary mass extinction (Dalrymple et al., 1993; Izett et al., 1991; Renne et al., 2013; Sharpton et al., 1992; Swisher et al., 1992), albeit with an error margin of 1%–2% due to argon loss, making such claims dubious at best (e.g., Vermeesch, 2015). Later, Renne et al. (2013) reported $^{40}Ar/^{39}Ar$ ages of 66.043 ± 0.043 Ma for the Cretaceous-Paleogene boundary and 66.038 ± 0.025 Ma for impact spherules from Haiti, implying that the impact and the Cretaceous-Paleogene boundary ages were statistically indistinguishable. More recently, Renne et al. (2018) reported an age of 66.051 ± 0.031 Ma for the Gorgonilla impact spherules, concluding that the spherule age, and thus impact age, is indistinguishable from the Cretaceous-Paleogene boundary. Nevertheless, it is important to note that, even though the Chicxulub impact and the Cretaceous-Paleogene boundary ages are statistically indistinguishable, the dating error range spans 120 k.y. (maximum age difference of 21 ± 60 k.y.; Renne et al., 2018), even without taking into account uncertainties of argon loss. Therefore, a Cretaceous-Paleogene boundary $^{39}Ar/^{40}Ar$ age for the Chicxulub impact remains questionable and not inconsistent with a zone CF1 age. Solving this age problem will necessitate U-Pb zircon dating of ash layers above and below primary, as well as reworked, Chicxulub impact spherule deposits.

Role of the Chicxulub Impact in the Cretaceous-Paleogene Boundary Mass Extinction

In addition to the age controversy, only minor faunal changes have been associated with the Chicxulub impact, despite being claimed the main trigger of the Cretaceous-Paleogene boundary mass extinction (Keller et al., 2009a, 2009b). In contrast, Deccan volcanism in India has recently gained attention as a potential contributor to this biotic crisis because: (1) magnetostratigraphy and U-Pb dating reveals that 80% of the total Deccan volume erupted in C29r (Chenet et al., 2007, 2008, 2009), spanning the last 300 k.y. of the Maastrichtian and 500 k.y. of the early Danian (Schoene et al., 2015); (2) a record of the mass extinction within Deccan intertrappean sediments between the longest lava flows on Earth suggests a direct cause-and-effect relationship between these events (Keller et al., 2011a); and (3) Deccan volcanism in C29r below the Cretaceous-Paleogene boundary has been directly linked to rapid climate changes (e.g., Li and Keller, 1998; MacLeod and Huber, 2001; Nordt et al., 2003; Wilf et al., 2003; Stüben et al., 2003; MacLeod et al., 2005) and ocean acidification (e.g., Font et al., 2014, 2016; Punekar et al., 2016). These advances challenge the long-held belief that the Chicxulub impact was the sole cause for the Cretaceous-Paleogene boundary mass extinction. Impact proponents reconcile these findings with the impact hypothesis by proposing that the impact could have triggered accelerated and intensified Deccan volcanic eruptions, ultimately leading to the mass extinction (Renne et al., 2015; Richards et al., 2015; Sprain et al., 2019). However, such a link has been previously shown to be unlikely (Meschede et al., 2011). Moreover, Deccan eruptions accelerated well before the mass extinction, which would contradict a Cretaceous-Paleogene boundary age for the Chicxulub impact (Schoene, 2018, personal commun.). For all these reasons, the age of the Chicxulub impact remains controversial, and its environmental consequences must be reassessed in view of the massive Deccan eruptions driving climate change and ocean acidification associated with the Cretaceous-Paleogene boundary mass extinction.

CONCLUSIONS

(1) The Cretaceous–Paleogene section on Gorgonilla Island, Colombia, consists of light gray-yellow calcareous siliceous mudstones (pelagic deposits) alternating with dark olive-brown litharenites (turbidites). A 3-cm-thick Chicxulub impact spherule-rich layer separates Maastrichtian and Danian sediments.

(2) The Cretaceous-Paleogene boundary is marked by a major hiatus spanning >250 k.y. from the upper part of planktic foraminiferal zone CF1 in the late Maastrichtian to zones P0, P1a(1), and the lower part of P1a(2) in the early Danian. Radiolarian biostratigraphy also records a Cretaceous-Paleogene boundary hiatus based on the absence of earliest Danian zone RP1.

(3) Above the Cretaceous-Paleogene boundary hiatus, Chicxulub impact spherules are reworked into early Danian sediments, similar to Chicxulub impact deposits in the Caribbean and North Atlantic. The spherule-rich layer has a clast-supported sedimentary fabric with normal gradation and contains abundant glass spherules, lithics (mostly volcanic), and Maastrichtian and Danian microfossils. These characteristics indicate deposition by turbiditic currents, similar to the turbiditic litharenites observed throughout the section; they rule out interpretation of primary spherule deposition at Gorgonilla.

ACKNOWLEDGMENTS

This study was based upon work supported by Princeton University, Geosciences Department Tuttle and Scott funds; and the U.S. National Science Foundation (NSF) through the Continental Dynamics Program and Sedimentary Geology and Paleontology Program under NSF grants EAR-0207407 and EAR-0447171. We thank Alexis Godet and another anonymous reviewer for their comments. We thank Parques Nacionales de Colombia for permission to do field work on Gorgona and Gorgonilla Islands and to take samples from the Gorgonilla Cretaceous-Paleogene section. Special thanks go to Hermann Bermúdez,

Liliana Bolívar, and Wolfgang Stinnesbeck for their help during field work in Colombia, and to Julieta Suriano for her insights and feedback on the lithological and sedimentological analyses.

REFERENCES CITED

Abramovich, S., and Keller, G., 2002, High stress late Maastrichtian paleoenvironment: Inference from planktonic foraminifera in Tunisia: Palaeogeography, Palaeoclimatology, Palaeoecology, v. 178, no. 3-4, p. 145–164, https://doi.org/10.1016/S0031-0182(01)00394-7.

Abramovich, S., and Keller, G., 2003, Planktonic foraminiferal response to the latest Maastrichtian abrupt warm event: A case study from South Atlantic DSDP Site 525A: Marine Micropaleontology, v. 48, no. 3-4, p. 225–249, https://doi.org/10.1016/S0377-8398(03)00021-5.

Abramovich, S., Almongi-Labin, A., and Benjamini, C., 1998, Decline of the Maastrichtian pelagic ecosystem based on planktic foraminifera assemblage changes: Implication for the terminal Cretaceous faunal crisis: Geology, v. 26, p. 63–66, https://doi.org/10.1130/0091-7613(1998)026<0063:DOTMPE>2.3.CO;2.

Abramovich, S., Keller, G., Adatte, T., Stinnesbeck, W., Hottinger, L., Stüben, D., Berner, Z., Ramanivosoa, B., and Randriamanantenasoa, A., 2003, Age and paleoenvironment of the Maastrichtian-Paleocene of the Mahajanga Basin, Madagascar: A multidisciplinary approach: Marine Micropaleontology, v. 47, p. 17–70, https://doi.org/10.1016/S0377-8398(02)00094-4.

Abramovich, S., Yovel-Corem, S., Almogi-Labin, A., and Benjamini, C., 2010, Global climate change and planktic foraminiferal response in the Maastrichtian: Paleoceanography, v. 25, PA2201, https://doi.org/10.1029/2009PA001843.

Abramovich, S., Keller, G., Berner, Z., Cymbalista, M., and Rak, C., 2011, Maastrichtian planktic foraminiferal biostratigraphy and paleoenvironment of Brazos River, Falls County, Texas, U.S.A., *in* Keller, G., and Adatte, T., eds., The End-Cretaceous Mass Extinction and the Chicxulub Impact in Texas: Society for Sedimentary Geology (SEPM) Special Publication 100, p. 123–156, https://doi.org/10.2110/sepmsp.100.123.

Adatte, T., Stinnesbeck, W., and Keller, G., 1996, Lithostratigraphic and mineralogic correlations of near-K/T boundary clastic sediments in NE Mexico: Implications for origin and nature of deposition, *in* Ryder, G., Fastovsky, D., and Gartner, S., eds., The Cretaceous-Tertiary Event and Other Catastrophes in Earth History: Geological Society of America Special Paper 307, p. 211–226, https://doi.org/10.1130/0-8137-2307-8.211.

Adatte, T., Keller, G., and Baum, R., 2011, Age and origins of the Chicxulub impact and sandstone complex, Brazos River, Texas: Evidence from lithostratigraphy and sedimentology, *in* Keller, G., and Adatte, T., eds., The End-Cretaceous Mass Extinction and the Chicxulub Impact in Texas: Society for Sedimentary Geology (SEPM) Special Publication 100, p. 43–80, https://doi.org/10.2110/sepmsp.100.043.

Alegret, L., Arenillas, I., Arz, J.A., Díaz, C., Grajales-Nishimura, J.M., Meléndez, A., Molina, E., Rojas, R., and Soria, A.R., 2005, Cretaceous-Paleogene boundary deposits at Loma Capiro, central Cuba: Evidence for the Chicxulub impact: Geology, v. 33, p. 721–724, https://doi.org/10.1130/G21573.1.

Alvarez, L.W., Alvarez, W., Asaro, F., and Michel, H.V., 1980, Extraterrestrial cause for the Cretaceous-Tertiary extinction: Science, v. 208, p. 1095–1108, https://doi.org/10.1126/science.208.4448.1095.

Alvarez, W., Smit, J., Lowrie, W., Asaro, F., Margolis, S.V., Claeys, P., Kastner, M., and Hildebrand, A.R., 1992, Proximal impact deposits at the Cretaceous-Tertiary boundary in the Gulf of Mexico: A restudy of DSDP Leg 77 Sites 536 and 540: Geology, v. 20, p. 697–700, https://doi.org/10.1130/0091-7613(1992)020<0697:PIDATC>2.3.CO;2.

Arenillas, I., Arz, J.A., Grajales-Nishimura, J.M., Murillo-Muñetón, G., Alvarez, W., Camargo-Zanoguera, A., Molina, E., and Rosales-Domínguez, C., 2006, Chicxulub impact event is Cretaceous/Paleogene boundary in age: New micropaleontological evidence: Earth and Planetary Science Letters, v. 249, p. 241–257, https://doi.org/10.1016/j.epsl.2006.07.020.

Bermúdez, H.D., García, J., Stinnesbeck, W., Keller, G., Rodríguez, J.V., Hanel, M., Hopp, J., Schwarz, W.H., Trieloff, M., Bolívar, L., and Vega, F.J., 2016, The Cretaceous-Palaeogene boundary at Gorgonilla Island, Colombia, South America: Terra Nova, v. 28, no. 1, p. 83–90, https://doi.org/10.1111/ter.12196.

Bouma, A.H., 1962, Sedimentology of Some Flysch Deposits. A Graphic Approach to Facies Interpretation: Amsterdam, Netherlands, Elsevier, 168 p.

Caldeira, K., and Rampino, M.R., 1993, Aftermath of the end-Cretaceous mass extinction: Possible biogeochemical stabilization of the carbon cycle and climate: Paleoceanography, v. 8, no. 4, p. 515–525, https://doi.org/10.1029/93PA01163.

Caldeira, K., Rampino, M.R., Volk, T., and Zachos, J.C., 1990, Biogeochemical modeling at mass extinction boundaries: Atmospheric carbon dioxide and ocean alkalinity at the K/T boundary, *in* Kauffman, E.G., and Walliser, O.K., eds., Global Bioevents: Abrupt Changes in the Global Biota Through Time: New York, Springer-Verlag, p. 333–345, https://doi.org/10.1007/BFb0011156.

Canudo, J.I., Keller, G., and Molina, E., 1991, Cretaceous/Tertiary boundary extinction pattern and faunal turnover at Agost and Caravaca, SE Spain: Marine Micropaleontology, v. 17, p. 319–341, https://doi.org/10.1016/0377-8398(91)90019-3.

Carracedo Sánchez, M., Arostegui, J., Sarrionandia, F., Larrondo, E., and Gil Ibarguchi, J.I., 2010, Cryptoachneliths: Hidden glassy ash in composite spheroidal lapilli: Journal of Volcanology and Geothermal Research, v. 196, p. 77–90, https://doi.org/10.1016/j.jvolgeores.2010.07.009.

Chenet, A.-L., Quidelleur, X., Fluteau, F., Courtillot, V., and Bajpai, S., 2007, $^{40}K/^{40}Ar$ dating of the main Deccan large igneous province: Further evidence of Cretaceous-Tertiary boundary age and short duration: Earth and Planetary Science Letters, v. 263, p. 1–15, https://doi.org/10.1016/j.epsl.2007.07.011.

Chenet, A.-L., Fluteau, F., Courtillot, V., Gérard, M., and Subbarao, K.V., 2008, Determination of rapid Deccan eruptions across the Cretaceous-Tertiary boundary using paleomagnetic secular variation: Results from a 1200-m-thick section in the Mahabaleshwar escarpment: Journal of Geophysical Research–Solid Earth, v. 113, B04101, https://doi.org/10.1029/2006JB004635.

Chenet, A.-L., Courtillot, V., Fluteau, F., Gerard, M., Quidelleur, X., Khadri, S.F.R., Subbarao, K.V., and Thordarson, T., 2009, Determination of rapid Deccan eruptions across the Cretaceous-Tertiary boundary using paleomagnetic secular variation: 2. Constraints from analysis of eight new sections and synthesis for a 3500-m-thick composite section: Journal of Geophysical Research, v. 114, B06103, https://doi.org/10.1029/2008JB005644.

Clyde, W.C., Ramezani, J., Johnson, K.R., Bowring, S.A., and Jones, M.M., 2016, Direct high-precision U-Pb geochronology of the end-Cretaceous extinction and calibration of Paleocene astronomical timescales: Earth and Planetary Science Letters, v. 452, p. 272–280, https://doi.org/10.1016/j.epsl.2016.07.041.

Dalrymple, B.G., Izett, G.A., Snee, L.W., and Obradovich, J.D., 1993, $^{40}Ar/^{39}Ar$ Age Spectra and Total Fusion Ages of Tektites from Cretaceous-Tertiary Boundary Sedimentary Rocks in the Beloc Formation, Haiti: U.S. Geological Survey Bulletin 2065, 20 p., https://pubs.usgs.gov/bul/2065/report.pdf.

Eiler, J.M., 2001, Oxygen isotope variations of basaltic lavas and upper mantle rocks: Reviews in Mineralogy and Geochemistry, v. 43, no. 1, p. 319–364, https://doi.org/10.2138/gsrmg.43.1.319.

Ekdale, A.A., and Stinnesbeck, W., 1998, Trace fossils in Cretaceous-Tertiary (KT) boundary beds in northeastern Mexico: Implications for sedimentation during the KT boundary event: Palaios, v. 13, no. 6, p. 593–602, https://doi.org/10.2307/3515350.

Estrada, J.J., and MacDonald, W.D., 1994, Andean accretionary Cretaceous terranes: Paleomagnetic evidence supporting large latitudinal displacement component at Gorgona Island, Colombia: Eos (Washington, D.C.), v. 75, p. 127.

Font, E., Fabre, S., Nédélec, A., Adatte, T., Keller, G., Veiga-Pires, C., Ponte, J., Mirão, J., Khozyem, H., and Spangenberg, J.E., 2014, Atmospheric halogen and acid rains during the main phase of Deccan eruptions: Magnetic and mineral evidence, *in* Keller, G., and Kerr, A.C., eds., Volcanism, Impacts, and Mass Extinctions: Causes and Effects: Geological Society of America Special Paper 505, p. 353–368, https://doi.org/10.1130/2014.2505(18).

Font, E., Adatte, T., Sial, A.N., de Lacerda, L.D., Keller, G., and Punekar, J., 2016, Mercury anomaly, Deccan volcanism, and the end-Cretaceous mass extinction: Geology, v. 44, no. 2, p. 171–174, https://doi.org/10.1130/G37451.1.

Glass, B.P., and Simonson, B.M., 2012, Distal impact ejecta layers: Spherules and more: Elements, v. 8, no. 1, p. 43–48, https://doi.org/10.2113/gselements.8.1.43.

Heiken, G.H., 1974, An Atlas of Volcanic Ash: Smithsonian Contribution to the Earth Sciences 12, 101 p.

Heymann, D., Yancey, T.E., Wolbach, W.S., Thiemens, M.H., Johnson, E.A., Roach, D., and Moecker, S., 1998, Geochemical markers of the Cretaceous-Tertiary boundary event at Brazos River, Texas, USA: Geochimica et Cosmochimica Acta, v. 62, no. 1, p. 173–181, https://doi.org/10.1016/S0016-7037(97)00330-X.

Hildebrand, A.R., Penfield, G.T., Kring, D.A., Pilkington, M., Camargo, A., Jacobsen, S.B., and Boynton, W.V., 1991, Chicxulub crater: A possible Cretaceous/Tertiary boundary impact crater on the Yucatan Peninsula, Mexico: Geology, v. 19, no. 9, p. 867–871, https://doi.org/10.1130/0091-7613(1991)019<0867:CCAPCT>2.3.CO;2.

Hollis, C.J., 1993, Latest Cretaceous to late Paleocene radiolarian biostratigraphy: A new zonation from the New Zealand region: Marine Micropaleontology, v. 21, p. 295–327, https://doi.org/10.1016/0377-8398(93)90024-R.

Hollis, C.J., 1997, Cretaceous-Paleocene Radiolaria from Eastern Marlborough, New Zealand: Institute of Geological and Nuclear Sciences Monograph 17, 152 p.

Hollis, C.J., 2003, The Cretaceous/Tertiary boundary event in New Zealand: Profiling mass extinction: New Zealand Journal of Geology and Geophysics, v. 46, no. 2, p. 307–321, https://doi.org/10.1080/00288306.2003.9515011.

Hollis, C.J., Strong, C.P., Rodgers, K.A., and Rogers, K.M., 2003, Paleoenvironmental changes across the Cretaceous/Tertiary boundary at Flaxbourne River and Woodside Creek, eastern Marlborough, New Zealand: New Zealand Journal of Geology and Geophysics, v. 46, no. 2, p. 177–197, https://doi.org/10.1080/00288306.2003.9515003.

Huber, B.T., MacLeod, K.G., and Tur, N.A., 2008, Chronostratigraphic framework for Upper Campanian-Maastrichtian sediments on the Blake Nose (subtropical North Atlantic): Journal of Foraminiferal Research, v. 38, p. 162–182, https://doi.org/10.2113/gsjfr.38.2.162.

Husson, D., Galbrun, B., Laskar, J., Hinnov, L.A., Thibault, N., Gardin, S., and Locklair, R.E., 2011, Astronomical calibration of the Maastrichtian (Late Cretaceous): Earth and Planetary Science Letters, v. 305, p. 328–340, https://doi.org/10.1016/j.epsl.2011.03.008.

Izett, G.A., 1991, Tektites in the Cretaceous-Tertiary boundary rocks on Haiti and their bearing on the Alvarez impact extinction hypothesis: Journal of Geophysical Research, v. 96, p. 20,879–20,905, https://doi.org/10.1029/91JE02249.

Izett, G.A., Maurrasse, F.J.M.R., Lichte, F.E., Meeker, G.P., and Bates, R., 1990, Tektites in Cretaceous-Tertiary Boundary Rocks on Haiti: U.S. Geological Survey Open-File Report 90–635, 31 p., https://pubs.usgs.gov/of/1990/0635/report.pdf, https://doi.org/10.3133/ofr90635.

Izett, G.A., Dalrymple, G.B., and Snee, L.W., 1991, $^{40}Ar/^{39}Ar$ age of Cretaceous-Tertiary boundary tektites from Haiti: Science, v. 252, no. 5012, p. 1539–1542, https://doi.org/10.1126/science.252.5012.1539.

Keller, G., 1988, Extinctions, survivorship and evolution across the Cretaceous/Tertiary boundary at El Kef,

Tunisia: Marine Micropaleontology, v. 13, p. 239–263, https://doi.org/10.1016/0377-8398(88)90005-9.

Keller, G., 1989, Extended K/T boundary extinctions and delayed populational change in planktic foraminiferal faunas from Brazos River, Texas: Paleoceanography, v. 4, no. 3, p. 287–332, https://doi.org/10.1029/PA004i003p00287.

Keller, G., 2001, The end-Cretaceous mass extinction in the marine realm: Year 2000 assessment: Planetary and Space Science, v. 49, no. 8, p. 817–830, https://doi.org/10.1016/S0032-0633(01)00032-0.

Keller, G., 2002, *Guembelitria* dominated late Maastrichtian planktic foraminiferal assemblages mimic early Danian in the Eastern Desert of Egypt: Marine Micropaleontology, v. 47, no. 1-2, p. 71–99, https://doi.org/10.1016/S0377-8398(02)00116-0.

Keller, G., 2007, Impact stratigraphy: Old principle, new reality, *in* Evans, K.R., Horton, J.W., and King, D.T., eds., The Sedimentary Record of Meteorite Impacts: Geological Society of America Special Paper 437, p. 147–178, https://doi.org/10.1130/2008.2437(09).

Keller, G., 2011, The Cretaceous-Tertiary mass extinction: Theories and controversies, *in* Keller, G., and Adatte, T., eds., The End-Cretaceous Mass Extinction and the Chicxulub Impact in Texas: Society for Sedimentary Geology (SEPM) Special Publication 100, p. 7–22, https://doi.org/10.2110/sepmsp.100.007.

Keller, G., 2012, The Cretaceous-Tertiary mass extinction, Chicxulub impact, and Deccan volcanism, *in* Talent, J.A., ed., Earth and Life: Extinction Intervals and Biogeographic Perturbations through Time: International Year of Planet Earth: Dordrecht, Netherlands, Springer, p. 759–793, https://doi.org/10.1007/978-90-481-3428-1_25.

Keller, G., 2014, Deccan volcanism, the Chicxulub impact and the end-Cretaceous mass extinction: Coincidence? Cause and effect?, *in* Keller, G., and Kerr, A.C., eds., Volcanism, Impacts, and Mass Extinctions: Causes and Effects: Geological Society of America Special Paper 505, p. 57–89, https://doi.org/10.1130/2014.2505(03).

Keller, G., and Abramovich, S., 2009, Lilliput effect in late Maastrichtian planktic foraminifera: Response to environmental stress: Palaeogeography, Palaeoclimatology, Palaeoecology, v. 284, p. 47–62, https://doi.org/10.1016/j.palaeo.2009.08.029.

Keller, G., and Benjamini, C., 1991, Paleoenvironment of the eastern Tethys in the early Danian: Palaios, v. 6, p. 439–464, https://doi.org/10.2307/3514984.

Keller, G., and Lindinger, M., 1989, Stable isotope, TOC and $CaCO_3$ record across the Cretaceous/Tertiary boundary at El Kef, Tunisia: Palaeogeography, Palaeoclimatology, Palaeoecology, v. 73, no. 3-4, p. 243–265, https://doi.org/10.1016/0031-0182(89)90007-2.

Keller, G., Stinnesbeck, W., Adatte, T., MacLeod, N., and Lowe, D.R., 1994a, Field Guide to Cretaceous-Tertiary Boundary Sections in Northeastern Mexico: Houston, Texas, Lunar and Planetary Institute Contribution 827, 110 p.

Keller, G., Stinnesbeck, W., and Lopez-Oliva, J.G., 1994b, Age, deposition and biotic effects of the Cretaceous/Tertiary boundary event at Mimbral, NE Mexico: Palaios, v. 9, p. 144–157, https://doi.org/10.2307/3515102.

Keller, G., Li, L., and MacLeod, N., 1996, The Cretaceous-Tertiary boundary stratotype section at El Kef, Tunisia: How catastrophic was the mass extinction?: Palaeogeography, Palaeoclimatology, Palaeoecology, v. 119, p. 221–254, https://doi.org/10.1016/0031-0182(95)00009-7.

Keller, G., Lopez-Oliva, J.G., Stinnesbeck, W., and Adatte, T., 1997a, Age, stratigraphy and deposition of near K/T siliciclastic deposits in Mexico: Relation to bolide impact?: Geological Society of America Bulletin, v. 109, p. 410–428, https://doi.org/10.1130/0016-7606(1997)109<0410:ASADON>2.3.CO;2.

Keller, G., Adatte, T., Hollis, C., Ordóñez, M., Zambrano, I., Jiménez, N., Stinnesbeck, W., Aleman, A., and Hale-Erlich, W., 1997b, The Cretaceous/Tertiary boundary event in Ecuador: Reduced biotic effects due to eastern boundary current setting: Marine Micropaleontology, v. 31, no. 3-4, p. 97–133, https://doi.org/10.1016/S0377-8398(96)00061-8.

Keller, G., Adatte, T., Stinnesbeck, W., Stüben, D., and Berner, Z., 2001, Age, chemo- and biostratigraphy of Haiti spherule-rich deposits: A multi-event KT scenario: Canadian Journal of Earth Sciences, v. 38, no. 2, p. 197–227, https://doi.org/10.1139/e00-087.

Keller, G., Adatte, T., Stinnesbeck, W., Affolter, M., Schilli, L., and Lopez-Oliva, J.G., 2002a, Multiple spherule layers in the late Maastrichtian of northeastern Mexico, *in* Koeberl, C., and MacLeod, K.G., eds., Catastrophic Events and Mass Extinctions: Impacts and Beyond: Geological Society of America Special Paper 356, p. 145–161, https://doi.org/10.1130/0-8137-2356-6.145.

Keller, G., Adatte, T., Tantawy, A.A., Stinnesbeck, W., Luciani, V., Karoui-Yaakoub, N., and Zaghbib-Turki, D., 2002b, Paleoecology of Cretaceous-Tertiary mass extinction in planktonic foraminifera: Palaeogeography, Palaeoclimatology, Palaeoecology, v. 178, p. 257–297, https://doi.org/10.1016/S0031-0182(01)00399-6.

Keller, G., Stinnesbeck, W., Adatte, T., and Stüben, D., 2003a, Multiple impacts across the Cretaceous-Tertiary boundary: Earth-Science Reviews, v. 62, p. 327–363, https://doi.org/10.1016/S0012-8252(02)00162-9.

Keller, G., Stinnesbeck, W., Adatte, T., Holland, B., Stüben, D., Harting, M., De Leon, C., and De La Cruz, J., 2003b, Spherule deposits in Cretaceous-Tertiary boundary sediments in Belize and Guatemala: Journal of the Geological Society [London], v. 160, p. 783–795, https://doi.org/10.1144/0016-764902-119.

Keller, G., Adatte, T., Stinnesbeck, W., Rebolledo-Vieyra, M., Urrutia Fucugauchi, J., Kramar, G., and Stüben, D., 2004a, Chicxulub predates the K/T boundary mass extinction: Proceedings of the National Academy of Sciences of the United States of America, v. 101, p. 3753–3758, https://doi.org/10.1073/pnas.0400396101.

Keller, G., Adatte, T., and Stinnesbeck, W., 2004b, More evidence that Chicxulub predates KT boundary: Meteoritics & Planetary Science, v. 39, p. 1127–1144, https://doi.org/10.1111/j.1945-5100.2004.tb01133.x.

Keller, G., Adatte, T., Berner, Z., Harting, M., Baum, G., Prauss, M., Tantawy, A.A., and Stüben, D., 2007, Chicxulub impact predates K-T boundary: New evidence from Texas: Earth and Planetary Science Letters, v. 255, p. 339–356, https://doi.org/10.1016/j.epsl.2006.12.026.

Keller, G., Adatte, T., Pardo, A., and Lopez-Oliva, J.G., 2009a, New evidence concerning the age and biotic effects of the Chicxulub impact in NE Mexico: Journal of the Geological Society [London], v. 166, no. 3, p. 393–411, https://doi.org/10.1144/0016-76492008-116.

Keller, G., Abramovich, S., Berner, Z., and Adatte, T., 2009b, Biotic effects of the Chicxulub impact, K-T catastrophe and sea level change in Texas: Palaeogeography, Palaeoclimatology, Palaeoecology, v. 271, no. 1-2, p. 52–68, https://doi.org/10.1016/j.palaeo.2008.09.007.

Keller, G., Bhowmick, P.K., Upadhyay, H., Dave, A., Reddy, A.N., Jaiprakash, B.C., and Adatte, T., 2011a, Deccan volcanism linked to the Cretaceous-Tertiary boundary (KTB) mass extinction: New evidence from ONGC wells in the Krishna-Godavari Basin, India: Journal of the Geological Society of India, v. 78, p. 399–428, https://doi.org/10.1007/s12594-011-0107-3.

Keller, G., Abramovich, S., Adatte, T., and Berner, Z., 2011b, Biostratigraphy, age of the Chicxulub impact, and depositional environment of the Brazos River KTB sequences, *in* Keller, G., and Adatte, T., eds., The End-Cretaceous Mass Extinction and the Chicxulub Impact in Texas: Society for Sedimentary Geology (SEPM) Special Publication 100, p. 81–122, https://doi.org/10.2110/sepmsp.100.081.

Keller, G., Adatte, T., Bhowmick, P.K., Upadhyay, H., Dave, A., Reddy, A.N., and Jaiprakash, B.C., 2012, Nature and timing of extinctions in Cretaceous-Tertiary planktic foraminifera preserved in Deccan intertrappean sediments of the Krishna-Godavari Basin, India: Earth and Planetary Science Letters, v. 341–344, p. 211–221, https://doi.org/10.1016/j.epsl.2012.06.021.

Keller, G., Khozyem, H.M., Adatte, T., Malarkodi, N., Spangenberg, J.E., and Stinnesbeck, W., 2013, Chicxulub impact spherules in the North Atlantic and Caribbean: Age constraints and Cretaceous-Tertiary boundary hiatus: Geological Magazine, v. 150, p. 885–907, https://doi.org/10.1017/S0016756812001069.

Keller, G., Punekar, J., and Mateo, P., 2016, Upheavals during the late Maastrichtian: Volcanism, climate and faunal events preceding the end-Cretaceous mass extinction: Palaeogeography, Palaeoclimatology, Palaeoecology, v. 441, p. 137–151, https://doi.org/10.1016/j.palaeo.2015.06.034.

Kennan, L., and Pindell, J.L., 2009, Dextral shear, terrane accretion and basin formation in the Northern Andes: Best explained by interaction with a Pacific-derived Caribbean plate?, *in* James, K., Lorente, M.A., and Pindell, J., eds., The Geology and Evolution of the Region between North and South America: Geological Society [London] Special Publication 328, p. 487–531, https://doi.org/10.1144/SP328.20.

Kerr, A.C., and Tarney, J., 2005, Tectonic evolution of the Caribbean and northwestern South America: The case for accretion of two Late Cretaceous oceanic plateaus: Geology, v. 33, no. 4, p. 269–272, https://doi.org/10.1130/G21109.1.

Koeberl, C., and Sigurdsson, H., 1992, Geochemistry of impact glasses from the K/T boundary in Haiti: Relation to smectites and a new type of glass: Geochimica et Cosmochimica Acta, v. 56, no. 5, p. 2113–2129, https://doi.org/10.1016/0016-7037(92)90333-E.

Kübler, B., 1987, Cristallinité de l'illite—Méthodes normalisées de préparation; méthode normalisée de mesure; méthode automatique normalisée de mesure: Neuchâtel, Switzerland, Cahiers de l'Institut de Géologie, Université de Neuchâtel, Suisse, Série ADX, v. 2, p. 1–10.

Kump, L., 1991, Interpreting carbon-isotope excursions: Strangelove oceans: Geology, v. 19, p. 299–302, https://doi.org/10.1130/0091-7613(1991)019<0299:ICIESO>2.3.CO;2.

Kump, L.R., and Arthur, M.A., 1999, Interpreting carbon-isotope excursions: Carbonates and organic matter: Chemical Geology, v. 161, p. 181–198, https://doi.org/10.1016/S0009-2541(99)00086-8.

Lamolda, M., Aguado, R., Maurrasse, F.J.M.R., and Peryt, D., 1997, El tránsito Cretácico-Terciario en Beloc, Haití: Registro micropaleontológico e implicaciones bioestratigráficas: Geogaceta, v. 22, p. 97–100.

Li, L., and Keller, G., 1998, Maastrichtian climate, productivity and faunal turnovers in planktic foraminifera in South Atlantic DSDP Sites 525A and 21: Marine Micropaleontology, v. 33, p. 55–86, https://doi.org/10.1016/S0377-8398(97)00027-3.

Lopez-Oliva, J.G., and Keller, G., 1996, Age and stratigraphy of near-K/T boundary clastic deposits in NE Mexico, *in* Ryder, G., Fastovsky, D., and Gartner, S., eds., The Cretaceous-Tertiary Event and Other Catastrophes in Earth History: Geological Society of America Special Paper 307, p. 227–242.

Luciani, V., 2002, High resolution planktonic foraminiferal analysis from the Cretaceous/Tertiary boundary at Ain Settara (Tunisia): Evidence of an extended mass extinction: Palaeogeography, Palaeoclimatology, Palaeoecology, v. 178, no. 3-4, p. 299–319, https://doi.org/10.1016/S0031-0182(01)00400-X.

MacLeod, K.G., and Huber, B.T., 2001, The Maastrichtian record at Blake Nose (western North Atlantic) and implications for global palaeoceanographic and biotic changes, *in* Kroon, D., Norris, R.D., and Klaus, A., eds., Western North Atlantic Palaeogene and Cretaceous Palaeoceanography: Geological Society [London] Special Publication 183, p. 111–130, https://doi.org/10.1144/GSL.SP.2001.183.01.06.

MacLeod, K.G., Huber, B.T., and Isaza-Londoño, C., 2005, North Atlantic warming during global cooling at the end of the Cretaceous: Geology, v. 33, p. 437–440, https://doi.org/10.1130/G21466.1.

MacLeod, K.G., Whitney, D.L., Huber, B.T., and Koeberl, C., 2007, Impact and extinction in remarkably complete Cretaceous-Tertiary boundary sections from Demerara Rise, tropical western North Atlantic: Geological Society of America Bulletin, v. 119, p. 101–115, https://doi.org/10.1130/B25955.1.

MacLeod, N., and Keller, G., 1991, Hiatus distribution and mass extinctions at the Cretaceous-Tertiary boundary:

Geology, v. 19, p. 497–501, https://doi.org/10.1130/0091-7613(1991)019<0497:HDAMEA>2.3.CO;2.

MacLeod, N., and Keller, G., 1994, Comparative biogeographic analysis of planktic foraminiferal survivorship across the Cretaceous/Tertiary boundary: Paleobiology, v. 20, p. 143–177, https://doi.org/10.1017/S0094837300012653.

Mateo, P., Keller, G., Adatte, T., and Spangenberg, J.E., 2016, Mass wasting and hiatuses during the Cretaceous-Tertiary transition in the North Atlantic: Relationship to the Chicxulub impact?: Palaeogeography, Palaeoclimatology, Palaeoecology, v. 441, p. 96–115, https://doi.org/10.1016/j.palaeo.2015.01.019.

Maurrasse, F.J.M.R., and Sen, G., 1991, Impacts, tsunamis, and the Haitian Cretaceous-Tertiary boundary layer: Science, v. 252, p. 1690–1693, https://doi.org/10.1126/science.252.5013.1690.

Melson, W.G., O'Hearn, T., and Fredriksson, K., 1988, Composition and origin of basaltic glass spherules in pelagic clay from the eastern Pacific: Marine Geology, v. 83, no. 1-4, p. 253–271, https://doi.org/10.1016/0025-3227(88)90061-8.

Meschede, M.A., Myhrvold, C.L., and Tromp, J., 2011, Antipodal focusing of seismic waves due to large meteorite impacts on Earth: Geophysical Journal International, v. 187, p. 529–537, https://doi.org/10.1111/j.1365-246X.2011.05170.x.

Mitchell, S.F., Ball, J.D., Crowley, S.F., Marshall, J.D., Paul, C.R.C., Veltkamp, C.J., and Samir, A., 1997, Isotope data from Cretaceous chalks and foraminifera: Environmental or diagenetic signals?: Geology, v. 25, p. 691–694, https://doi.org/10.1130/0091-7613(1997)025<0691:IDFCCA>2.3.CO;2.

Molina, E., Arenillas, I., and Arz, J.A., 1998, Mass extinction in planktic foraminifera at the Cretaceous/Tertiary boundary in subtropical and temperate latitudes: Bulletin de la Société Géologique de France, v. 169, no. 3, p. 351–363.

Nederbragt, A.J., 1991, Late Cretaceous biostratigraphy and development of Heterohelicidae (planktic foraminifera): Micropaleontology, v. 37, p. 329–372, https://doi.org/10.2307/1485910.

Nichols, G., 2009, Sedimentology and Stratigraphy (2nd ed.): London, Wiley-Blackwell, 432 p.

Nordt, L., Atchley, S., and Dworkin, S., 2003, Terrestrial evidence for two greenhouse events in the latest Cretaceous: GSA Today, v. 13, p. 4–9, https://doi.org/10.1130/1052-5173(2003)013<4:TEFTGE>2.0.CO;2.

Norris, R.D., Huber, B.T., and Self-Trail, J., 1999, Synchroneity of the K-T oceanic mass extinction and meteorite impact: Blake Nose, western North Atlantic: Geology, v. 27, p. 419–422, https://doi.org/10.1130/0091-7613(1999)027<0419:SOTKTO>2.3.CO;2.

Norris, R.D., Firth, J., Blusztajn, J., and Ravizza, G., 2000, Mass failure of the North Atlantic margin triggered by the Cretaceous-Paleogene bolide impact: Geology, v. 28, p. 1119–1122, https://doi.org/10.1130/0091-7613(2000)28<1119:MFOTNA>2.0.CO;2.

Olsson, R.K., Miller, K.G., Browning, J.V., Habib, D., and Sugarmann, P.J., 1997, Ejecta layer at the Cretaceous-Tertiary boundary, Bass River, New Jersey (Ocean Drilling Program Leg 174AX): Geology, v. 25, p. 759–762, https://doi.org/10.1130/0091-7613(1997)025<0759:ELATCT>2.3.CO;2.

Olsson, R.K., Hemleben, C., Berggren, W.A., and Huber, B.T., 1999, Atlas of Paleocene Planktonic Foraminifera: Smithsonian Contributions to Paleobiology 85, 252 p.

Pardo, A., and Keller, G., 2008, Biotic effects of environmental catastrophes at the end of the Cretaceous: *Guembelitria* and *Heterohelix* blooms: Cretaceous Research, v. 29, no. 5-6, p. 1058–1073, https://doi.org/10.1016/j.cretres.2008.05.031.

Pardo, A., Ortiz, N., and Keller, G., 1996, Latest Maastrichtian and K/T boundary foraminiferal turnover and environmental changes at Agost, Spain, *in* MacLeod, N., and Keller, G., eds., The Cretaceous/Tertiary Mass Extinction: Biotic and Environmental Events: New York, W.W. Norton and Co., p. 155–176.

Pope, K.O., Ocampo, A.C., and Duller, C.E., 1991, Mexican site for K/T impact crater?: Nature, v. 351, p. 105, https://doi.org/10.1038/351105a0.

Punekar, J., Mateo, P., and Keller, G., 2014a, Environmental and biological effects of Deccan volcanism: A global survey, *in* Keller, G., and Kerr, A.C., eds., Volcanism, Impacts, and Mass Extinctions: Causes and Effects: Geological Society of America Special Paper 505, p. 91–116, https://doi.org/10.1130/2014.2505(04).

Punekar, J., Keller, G., Khozyem, H.M., Hamming, C., Adatte, T., Tantawy, A.A., and Spangenberg, J., 2014b, Late Maastrichtian–early Danian high-stress environments and delayed recovery linked to Deccan volcanism: Cretaceous Research, v. 49, p. 63–82, https://doi.org/10.1016/j.cretres.2014.01.002.

Punekar, J., Keller, G., Khozyem, H.M., Adatte, T., Font, E., and Spangenberg, J., 2016, A multi-proxy approach to decode the end-Cretaceous mass extinction: Palaeogeography, Palaeoclimatology, Palaeoecology, v. 441, p. 116–136, https://doi.org/10.1016/j.palaeo.2015.08.025.

Quillévéré, F., Norris, R.D., Kroon, D., and Wilson, P.A., 2008, Transient ocean warming and shifts in carbon reservoirs during the early Danian: Earth and Planetary Science Letters, v. 265, p. 600–615, https://doi.org/10.1016/j.epsl.2007.10.040.

Reineck, H.E., and Singh, I.B., 1980, Depositional Sedimentary Environments, with Reference to Terrigenous Clastics (2nd ed.): Berlin, Springer-Verlag, 551 p.

Renne, P.R., Deino, A.L., Hilgen, F.J., Kuiper, K.F., Mark, D.F., Mitchell, W.S., III, Morgan, L.E., Mundil, R., and Smit, J., 2013, Time scales of critical events around the Cretaceous-Paleogene boundary: Science, v. 339, p. 684–687, https://doi.org/10.1126/science.1230492.

Renne, P.R., Sprain, C.J., Richards, M.A., Self, S., Vanderkluysen, L., and Pande, K., 2015, State shift in Deccan volcanism at the Cretaceous-Paleogene boundary, possibly induced by impact: Science, v. 350, no. 6256, p. 76–78, https://doi.org/10.1126/science.aac7549.

Renne, P.R., Arenillas, I., Arz, J.A., Vajda, V., Gilabert, V., and Bermúdez, H.D., 2018, Multi-proxy record of the Chicxulub impact at the Cretaceous-Paleogene boundary from Gorgonilla Island, Colombia: Geology, v. 46, no. 6, p. 547–550, https://doi.org/10.1130/G40224.1.

Richards, M.A., Alvarez, W., Self, S., Karlstrom, L., Renne, P.R., Manga, M., Sprain, C.J., Smit, J., Vanderkluysen, L., and Gibson, S.A., 2015, Triggering of the largest Deccan eruptions by the Chicxulub impact: Geological Society of America Bulletin, v. 127, no. 11-12, p. 1507–1520, https://doi.org/10.1130/B31167.1.

Robaszynski, F., Caron, M., Gonzalez Donoso, J.M., and Wonders, A.A.H., 1983–1984, Atlas of Late Cretaceous globotruncanids: Micropaleontology, v. 26, no. 3-4, p. 145–305.

Schoene, B., Samperton, K.M., Eddy, M.P., Keller, G., Adatte, T., Bowring, S.A., Khadri, S.F.R., and Gertsch, B., 2015, U-Pb geochronology of the Deccan Traps and relation to the end-Cretaceous mass extinction: Science, v. 347, p. 182–184, https://doi.org/10.1126/science.aaa0118.

Schoene, B., Eddy, M.P., Samperton, K.M., Keller, C.B., Keller, G., Adatte, T., and Khadri, S.F., 2019, U-Pb constraints on pulsed eruption of the Deccan Traps across the end-Cretaceous mass extinction: Science, v. 363, p. 862–866, https://doi.org/10.1126/science.aau2422.

Schulte, P., Stinnesbeck, W., Stüben, D., Kramar, U., Berner, Z., Keller, G., and Adatte, T., 2003, Fe-rich and K-rich mafic spherules from slumped and channelized Chicxulub ejecta deposits in the northern La Sierrita area, NE Mexico: International Journal of Earth Sciences, v. 92, p. 114–142, https://doi.org/10.1007/s00531-002-0304-9.

Schulte, P., Speijer, R.P., Mai, H., and Kontny, A., 2006, The Cretaceous-Paleogene (K-P) boundary at Brazos, Texas: Sequence stratigraphy, depositional events and the Chicxulub impact: Sedimentary Geology, v. 184, p. 77–109, https://doi.org/10.1016/j.sedgeo.2005.09.021.

Schulte, P., Deutsch, A., Salge, T., Berndt, J., Kontny, A., MacLeod, K., Neuser, R.D., and Krumm, S., 2009, A dual-layer Chicxulub ejecta sequence with shocked carbonates from the Cretaceous-Paleogene (K-Pg) boundary, Demerara Rise, western Atlantic: Geochimica et Cosmochimica Acta, v. 73, p. 1180–1204, https://doi.org/10.1016/j.gca.2008.11.011.

Schulte, P., Alegret, L., Arenillas, I., Arz, J.A., Barton, P.J., Bown, P.R., Bralower, T.J., Christeson, G.L., Claeys, P., Cockell, C.S., Collins, G.S., Deutsch, A., Goldin, T.J., Goto, K., Grajales-Nishimura, J.M., Grieve, R.A.F., Gulick, S.P.S., Johnson, K.R., Kiessling, W., Koeberl, C., Kring, D.A., MacLeod, K.G., Matsui, T., Melosh, J., Montanari, A., Morgan, J.V., Neal, C.R., Nichols, D.J., Norris, R.D., Pierazzo, E., Ravizza, G., Rebolledo-Vieyra, M., Reimold, W.U., Robin, E., Salge, T., Speijer, R.P., Sweet, A.R., Urrutia-Fucugauchi, J., Vajda, V., Whalen, M.T., and Willumsen, P.S., 2010, The Chicxulub asteroid impact and mass extinction at the Cretaceous-Paleogene boundary: Science, v. 327, p. 1214–1218, https://doi.org/10.1126/science.1177265.

Serrano, L., Ferrari, L., Martínez, M.L., Petrone, C.M., and Jaramillo, C., 2011, An integrative geologic, geochronologic and geochemical study of Gorgona Island, Colombia: Implications for the formation of the Caribbean large igneous province: Earth and Planetary Science Letters, v. 309, no. 3-4, p. 324–336, https://doi.org/10.1016/j.epsl.2011.07.011.

Sharpton, V.L., Dalrymplei, G.B., Maríni, L.E., Ryder, G., Schuraytz, B.C., and Urrutia-Fucugauchi, J., 1992, New links between the Chicxulub impact structure and the Cretaceous/Tertiary boundary: Nature, v. 359, p. 819–821, https://doi.org/10.1038/359819a0.

Sigurdsson, H., D'Hondt, S., Arthur, M.A., Bralower, T.J., Zachos, J.C., Van Fossen, M., and Channell, J.E.T., 1991, Glass from the Cretaceous-Tertiary boundary in Haiti: Nature, v. 349, p. 482–487, https://doi.org/10.1038/349482a0.

Smit, J., 1999, The global stratigraphy of the Cretaceous-Tertiary boundary impact ejecta: Annual Review of Earth and Planetary Sciences, v. 27, no. 1, p. 75–113, https://doi.org/10.1146/annurev.earth.27.1.75.

Smit, J., Montanari, A., Swinburne, N.H.M., Alvarez, W., Hildebrand, A.R., Margolis, S.V., Claeys, P., Lowrie, W., and Asaro, F., 1992, Tektite-bearing, deep-water clastic unit at the Cretaceous-Tertiary boundary in northeastern Mexico: Geology, v. 20, p. 99–103, https://doi.org/10.1130/0091-7613(1992)020<0099:TBDWCU>2.3.CO;2.

Smit, J., Roep, T.B., Alvarez, W., Montanari, A., Claeys, P., Grajales Nishimura, J.M., and Bermudez, J., 1996, Coarse-grained clastic sandstone complex at the K/T boundary around the Gulf of Mexico: Deposition by tsunami waves induced by the Chicxulub impact?, *in* Ryder, G., Fastovsky, D., and Gartner, S., eds., The Cretaceous-Tertiary Event and Other Catastrophes in Earth History: Geological Society of America Special Paper 307, p. 151–182, https://doi.org/10.1130/0-8137-2307-8.151.

Soria, A.R., Liesa, C.L., Mata, M.P., Arz, J.A., Alegret, L., Arenillas, I., and Meléndez, A., 2001, Slumping and a sandbar deposit at the Cretaceous-Tertiary boundary in the El Tecolote section (northeastern Mexico): An impact-induced sediment gravity flow: Geology, v. 29, no. 3, p. 231–234, https://doi.org/10.1130/0091-7613(2001)029<0231:SAASDA>2.0.CO;2.

Spötl, C., and Vennemann, T.W., 2003, Continuous-flow isotope ratio mass spectrometric analysis of carbonate minerals: Rapid Communications in Mass Spectrometry, v. 17, p. 1004–1006, https://doi.org/10.1002/rcm.1010.

Sprain, C.J., Renne, P.R., Vanderkluysen, L., Pande, K., Self, S., and Mittal, T., 2019, The eruptive tempo of Deccan volcanism in relation to the Cretaceous-Paleogene boundary: Science, v. 363, p. 866–870, https://doi.org/10.1126/science.aav1446.

Stinnesbeck, W., Barbarin, J.M., Keller, G., Lopez-Oliva, J.G., Pivnik, D.A., Lyons, J.B., Officer, C.B., Adatte, T., Graup, G., Rocchia, R., and Robin, E., 1993, Deposition of channel deposits near the Cretaceous-Tertiary boundary in northeastern Mexico: Catastrophic or "normal" sedimentary deposits: Geology, v. 21, p. 797–800, https://doi.org/10.1130/0091-7613(1993)021<0797:DOCDNT>2.3.CO;2.

Stinnesbeck, W., Keller, G., Adatte, T., Lopez-Oliva, J.G., and Macleod, N., 1996, Cretaceous-Tertiary boundary clastic deposits in northeastern Mexico: Impact tsunami or sea level lowstand?, *in* MacLeod, N., and

Keller, G., eds., Cretaceous-Tertiary Mass Extinctions: Biotic and Environmental Changes: New York, W.W. Norton, p. 471–518.

Stinnesbeck, W., Keller, G., de la Cruz, J., DeLeon, C., Macleod, N., and Whittaker, J.E., 1997, The Cretaceous-Tertiary boundary in Guatemala—Limestone breccia deposits from the South Peten Basin: Geologische Rundschau, v. 86, no. 3, p. 686–709, https://doi.org/10.1007/s005310050171.

Storey, M., Mahoney, J.J., Kroenke, L.W., and Saunders, A.D., 1991, Are oceanic plateaus sites of komatiite formation?: Geology, v. 19, p. 376–379, https://doi.org/10.1130/0091-7613(1991)019<0376:AOPSOK>2.3.CO;2.

Stüben, D., Kramar, U., Berner, Z., Stinnesbeck, W., Keller, G., and Adatte, T., 2002, Trace elements, stable isotopes, and clay mineralogy of the Elles II K-T boundary section in Tunisia: Indications for sea level fluctuations and primary productivity: Palaeogeography, Palaeoclimatology, Palaeoecology, v. 178, no. 3-4, p. 321–345, https://doi.org/10.1016/S0031-0182(01)00401-1.

Stüben, D., Kramar, U., Berner, Z.A., Meudt, M., Keller, G., Abramovich, S., Adatte, T., Hambach, U., and Stinnesbeck, W., 2003, Late Maastrichtian paleoclimatic and paleoceanographic changes inferred from Sr/Ca ratio and stable isotopes: Palaeogeography, Palaeoclimatology, Palaeoecology, v. 199, p. 107–127, https://doi.org/10.1016/S0031-0182(03)00499-1.

Swisher, C.C., III, Grajales-Nishimura, J.M., Montanari, A., Margolis, S.V., Claeys, P., Alvarez, W., Renne, P., Cedillo-Pardo, E., Maurrasse, F.J.R., Curtis, G.H., and Smit, J., 1992, Coeval $^{40}Ar/^{39}Ar$ ages of 65.0 million years ago from Chicxulub crater melt rock and Cretaceous-Tertiary boundary tektites: Science, v. 257, no. 5072, p. 954–958, https://doi.org/10.1126/science.257.5072.954.

Vallier, T.L., Bohrer, D., Moreland, G., and McKee, E.H., 1977, Origin of basalt microlapilli in Lower Miocene pelagic sediment, northeastern Pacific Ocean: Geological Society of America Bulletin, v. 88, no. 6, p. 787–796, https://doi.org/10.1130/0016-7606(1977)88<787:OOBMIL>2.0.CO;2.

Van Fossen, M.C., Channell, F.E.T., and Bralower, T.J., 1995, Geomagnetic polarity stratigraphy and nannofossil biostratigraphy at the K/T boundary section near Beloc, Haiti: Cretaceous Research, v. 16, p. 131–139, https://doi.org/10.1006/cres.1995.1008.

Vennemann, T.W., Morlok, A., von Engelhardt, W.E., and Kyser, T.K., 2001, Stable isotope composition of impact glasses from the Nördlinger Ries impact crater, Germany: Geochimica et Cosmochimica Acta, v. 65, no. 8, p. 1325–1336, https://doi.org/10.1016/S0016-7037(00)00600-1.

Vermeesch, P., 2015, Revised error propagation of $^{40}Ar/^{39}Ar$ data, including covariances: Geochimica et Cosmochimica Acta, v. 171, p. 325–337, https://doi.org/10.1016/j.gca.2015.09.008.

Walker, G.P.L., and Croasdale, R., 1971, Characteristics of some basaltic pyroclasts: Bulletin of Volcanology, v. 35, p. 303–317, https://doi.org/10.1007/BF02596957.

Wilf, P., Johnson, K.R., and Huber, B.T., 2003, Correlated terrestrial and marine evidence for global climate changes before mass extinction at the Cretaceous-Paleogene boundary: Proceedings of the National Academy of Sciences of the United States of America, v. 100, no. 2, p. 599–604, https://doi.org/10.1073/pnas.0234701100.

Yancey, T.E., 1996, Stratigraphy and depositional environments of the Cretaceous-Tertiary boundary complex and basal Paleocene section, Brazos River, Texas: Gulf Coast Association of Geological Societies Transactions, v. 46, p. 433–442.

Science Editor: Rob Strachan

Manuscript Received by the Society 11 March 2019
Revised Manuscript Received 15 March 2019
Manuscript Accepted 29 April 2019

Printed in the USA